Supporting Information (SI)

Donepezil-Based Rational Design of *N*-Substituted Quinazolinthioacetamide Candidates as Potential Acetylcholine Esterase Inhibitors for the Treatment of Alzheimer's Disease: *In vitro* and *In vivo* Studies

Ahmed A. Al-Karmalawy[1,2,*], Ahmed F. Mohamed[3,4], Heba Nasr Shalaby[3], Ayman Abo Elmaaty[5,6], Riham A. El-Shiekh[7], Mohamed A. Zeidan[2], Radwan Alnajjar[8], Abdullah Yahya Abdullah Alzahrani[9], Mohammed H. AL Mughram[10], Moataz A. Shaldam[11], Haytham O. Tawfik[12,*]

[1] Department of Pharmaceutical Chemistry, College of Pharmacy, The University of Mashreq, Baghdad 10023, Iraq.

[2] Department of Pharmaceutical Chemistry, Faculty of Pharmacy, Horus University-Egypt, New Damietta 34518, Egypt.

[3] Department of Pharmacology and Toxicology, Faculty of Pharmacy, Cairo University, Cairo, Egypt.

[4] Faculty of Pharmacy, King Salman International University (KSIU), South Sinai 46612, Egypt.

[5] Medicinal Chemistry Department, Faculty of Pharmacy, Port Said University, Port Said 42526, Egypt.

[6] Medicinal Chemistry Department, Clinical Pharmacy Program, East Port said National University, Port Said 42526, Egypt.

[7] Pharmacognosy Department, Faculty of Pharmacy, Cairo University, Kasr-El-Ainy Street, Cairo 11562, Egypt.

[8] CADD Unit, Faculty of Pharmacy, Libyan International Medical University, Benghazi 16063, Libya.

[9] Department of Chemistry, Faculty of Science and Arts, King Khalid University, Mohail Assir, Saudi Arabia.

[10] Department of Pharmaceutical Chemistry, College of Pharmacy, King Khalid University, Abha 61421, Saudi Arabia.

[11] Department of Pharmaceutical Chemistry, Faculty of Pharmacy, Kafrelsheikh University, Kafrelsheikh 33516, Egypt

[12] Department of Pharmaceutical Chemistry, Faculty of Pharmacy, Tanta University, Tanta 31527, Egypt.

*Corresponding authors:

Ahmed A. Al-Karmalawy; Email: akarmalawy@horus.edu.eg

Haytham O. Tawfik; Email: haytham.omar.mahmoud@pharm.tanta.edu.eg

Table of Contents

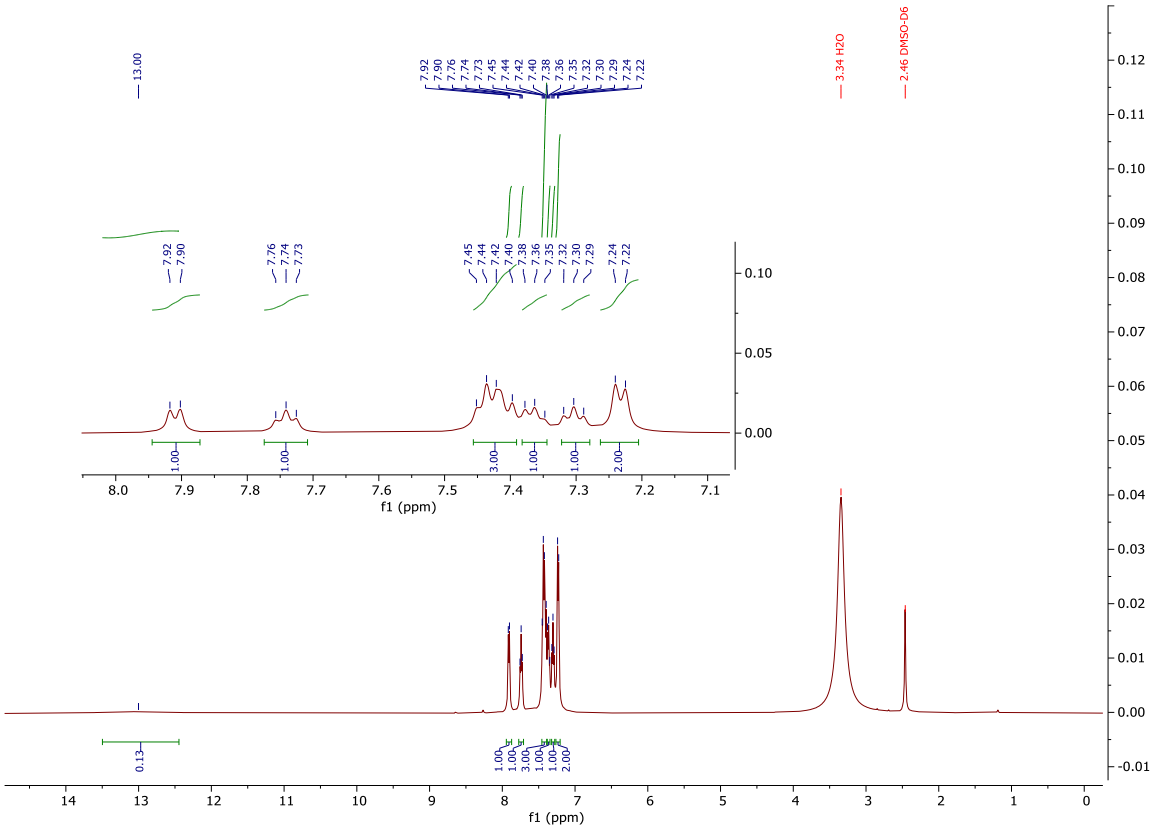

Figure S1. ^{1}H NMR spectrum (500 MHz, DMSO-d_6) for intermediate **1**.

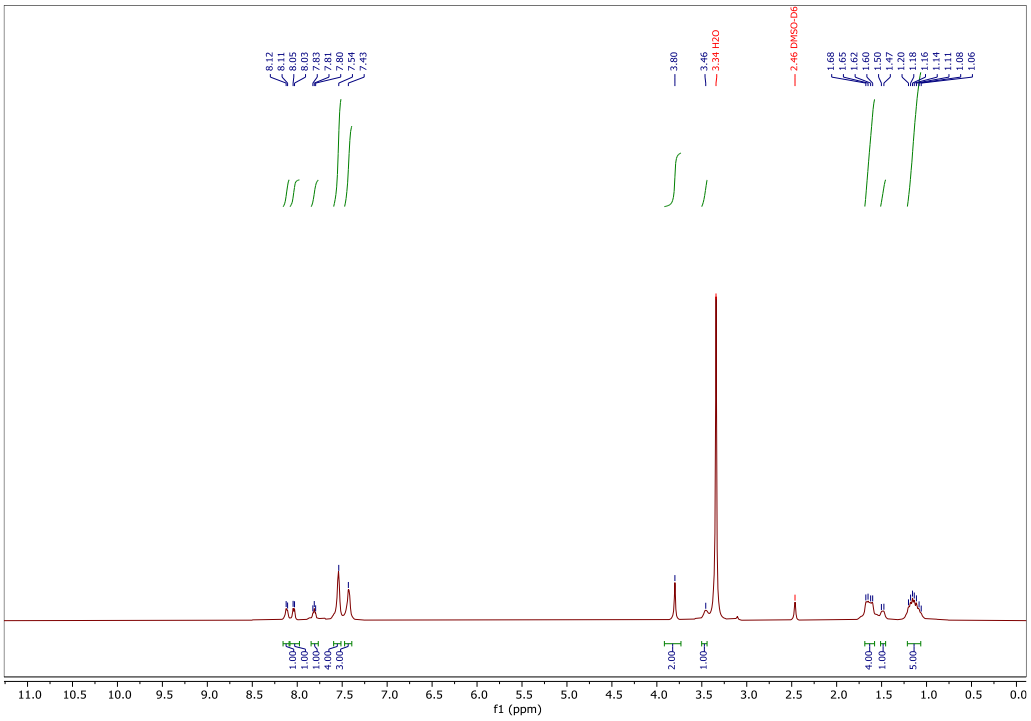

Figure S2. ^{1}H NMR spectrum (500 MHz, DMSO-d_6) for compound **3a**.

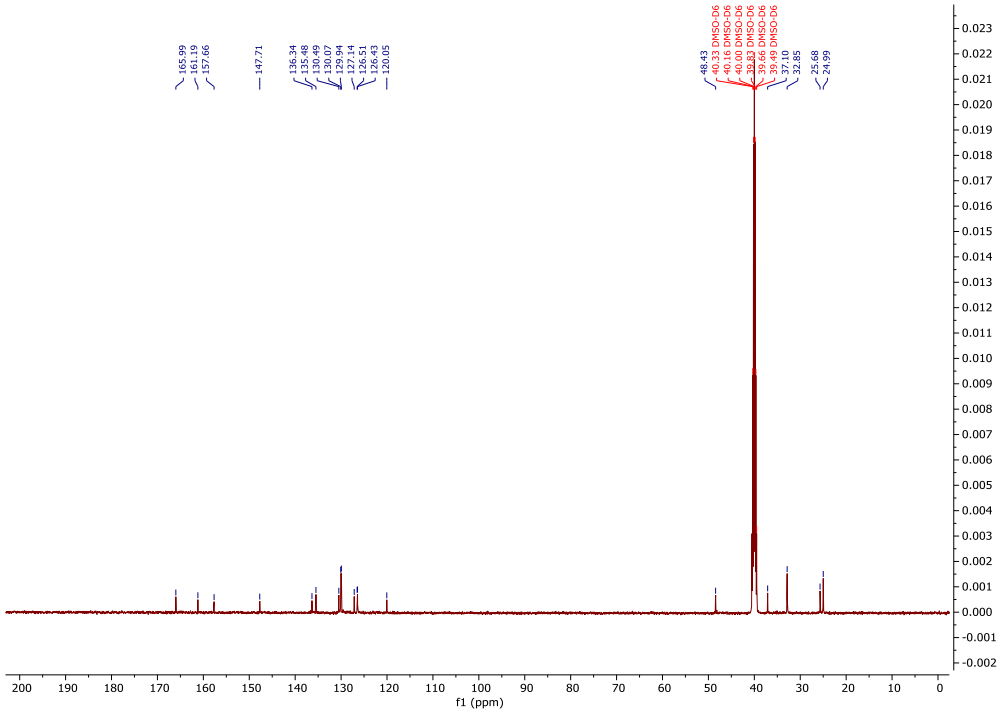

Figure S3. ^{13}C NMR spectrum (125 MHz, DMSO-d_6) for compound **3a**.

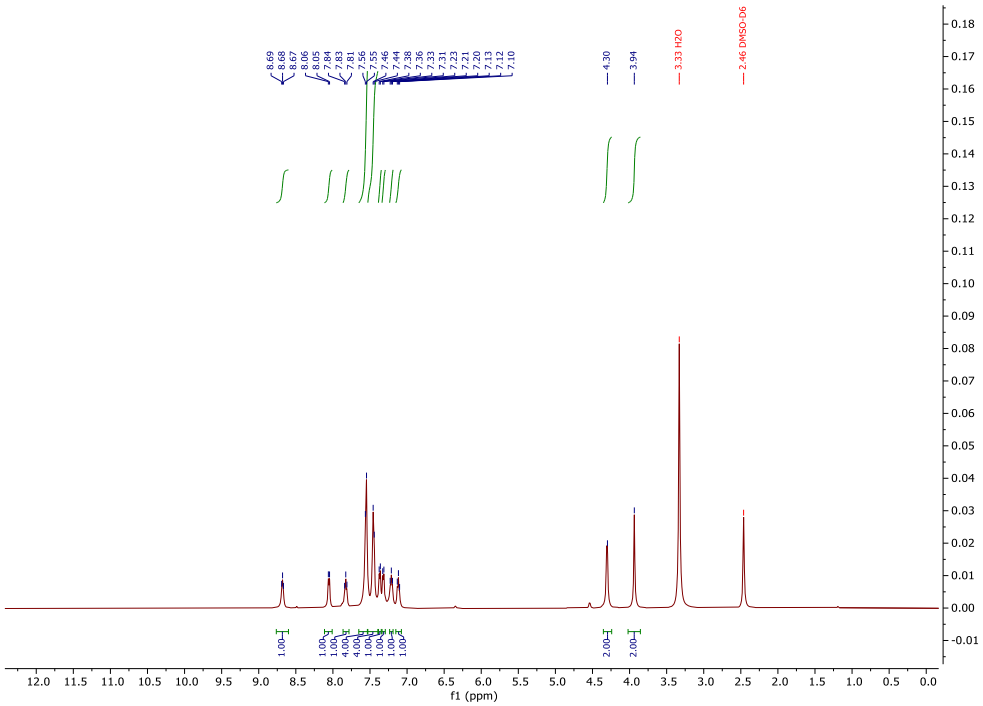

Figure S4. ^{1}H NMR spectrum (500 MHz, DMSO-d_6) for compound **3b**.

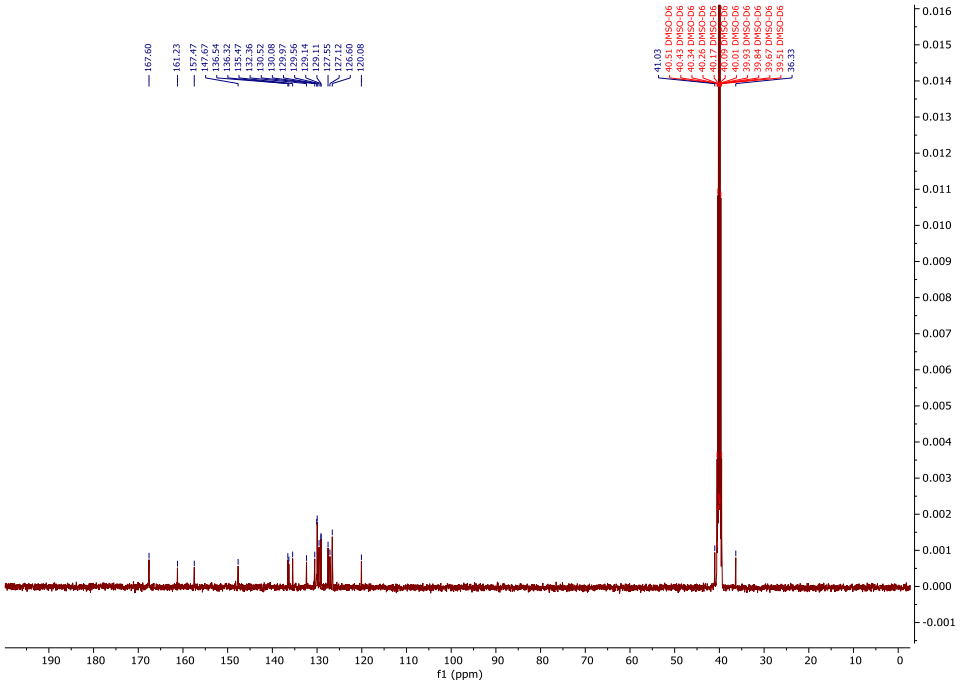

Figure S5. ^{13}C NMR spectrum (125 MHz, DMSO-d_6) for compound **3b**.

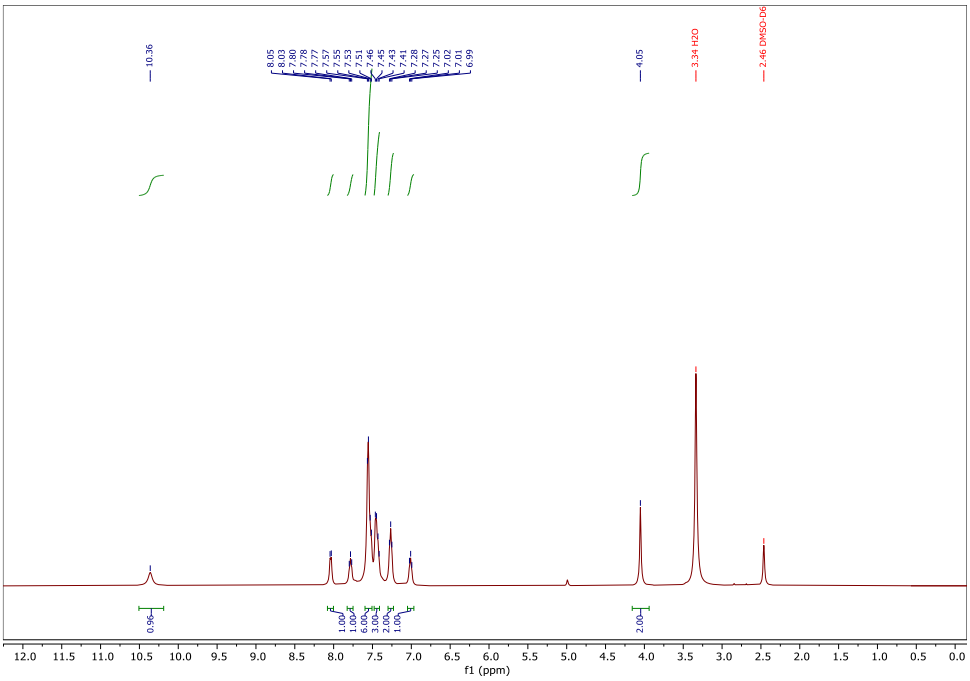

Figure S6. ^{1}H NMR spectrum (500 MHz, DMSO-d_6) for compound **3c**.

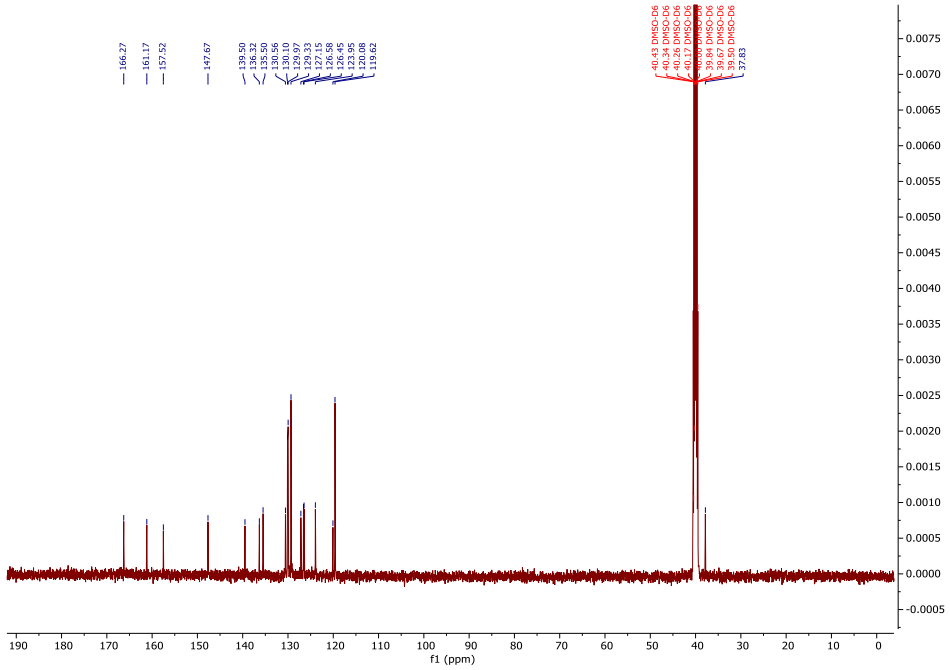

Figure S7. ^{13}C NMR spectrum (125 MHz, DMSO-d_6) for compound **3c**.

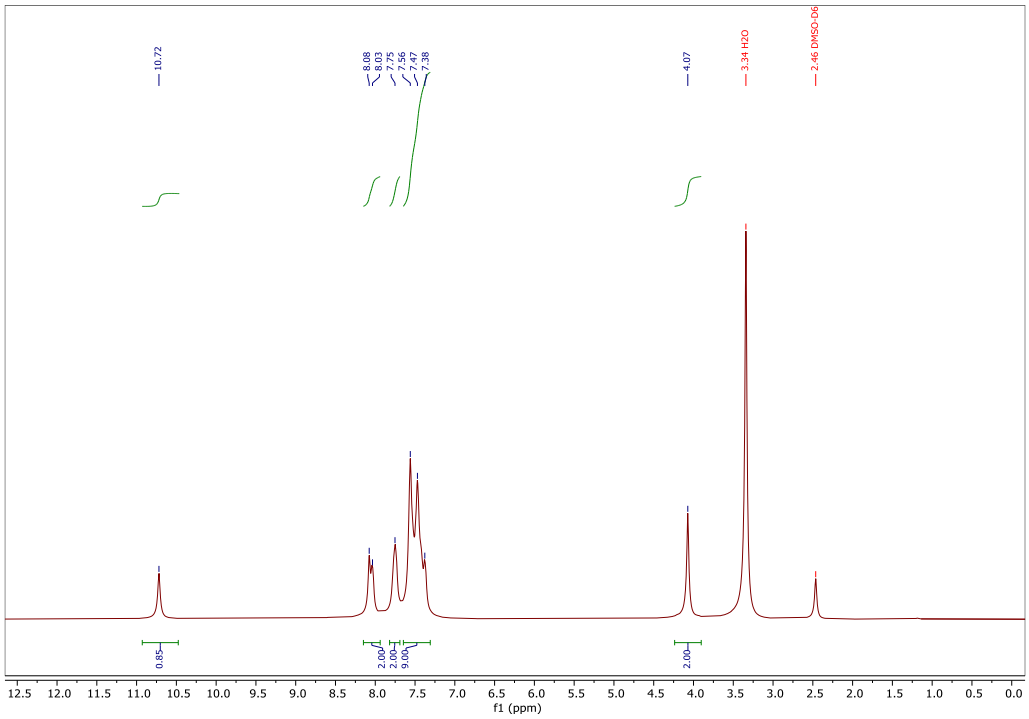

Figure S8. ^{1}H NMR spectrum (500 MHz, DMSO-d_6) for compound **3d**.

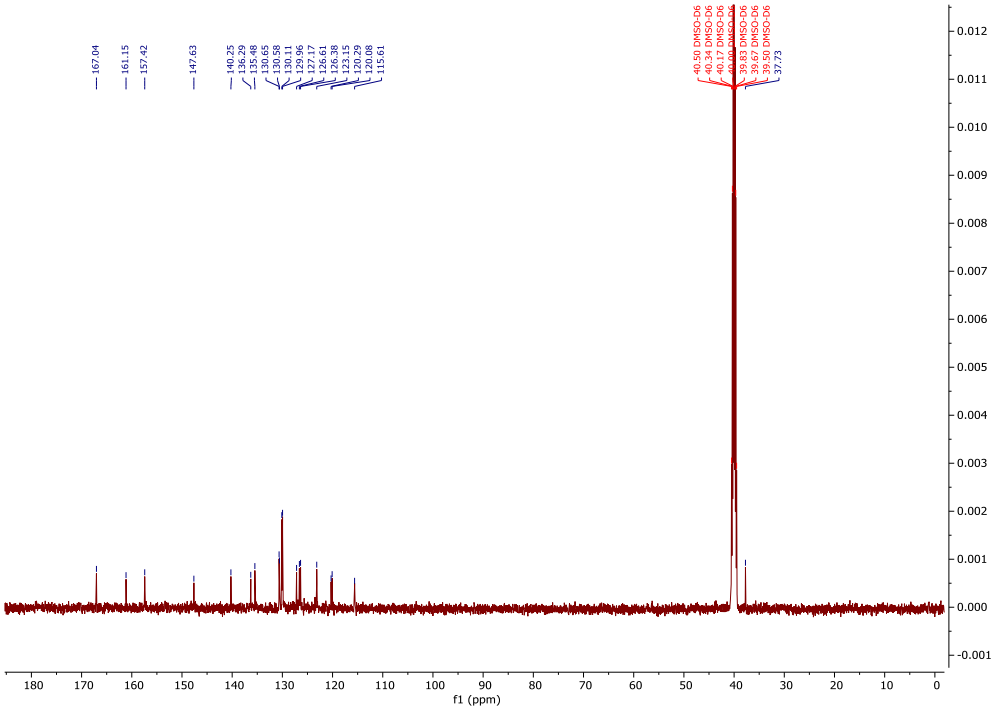

Figure S9. ^{13}C NMR spectrum (125 MHz, DMSO-d_6) for compound **3d**.

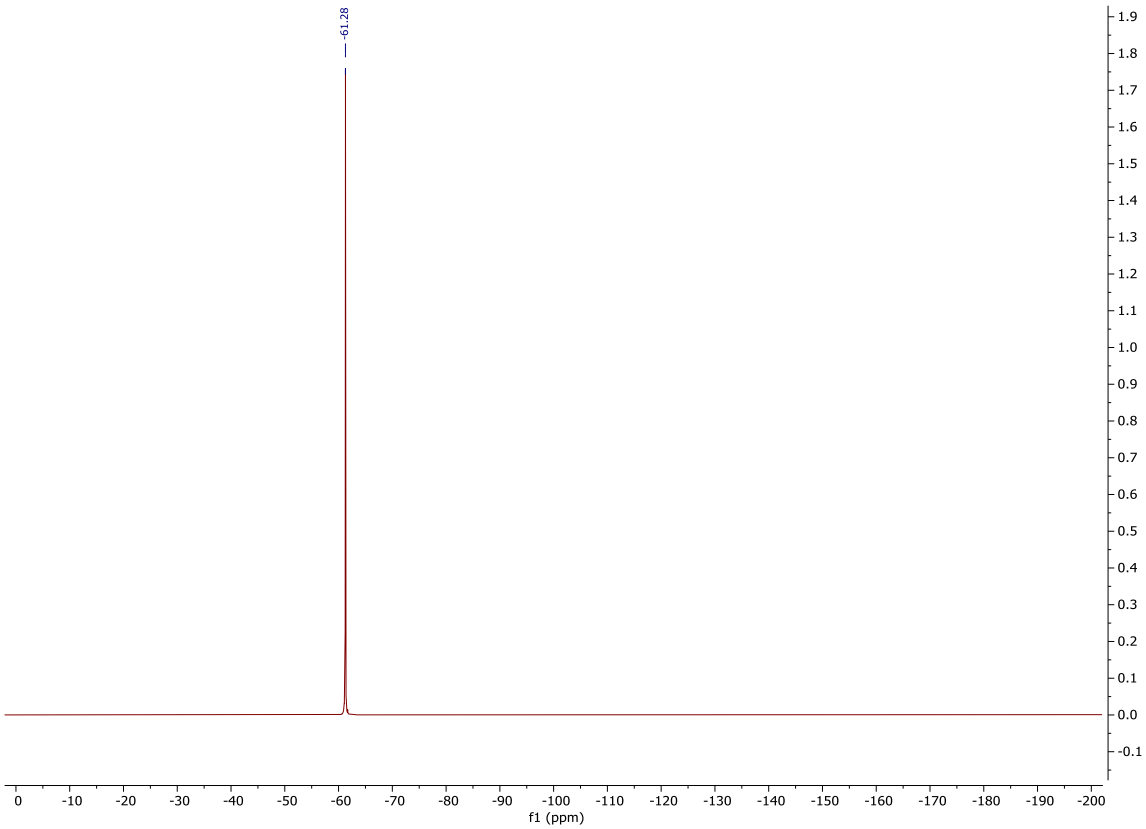

Figure S10. ^{19}F NMR spectrum (471 MHz, DMSO-d_6) for compound **3d**.

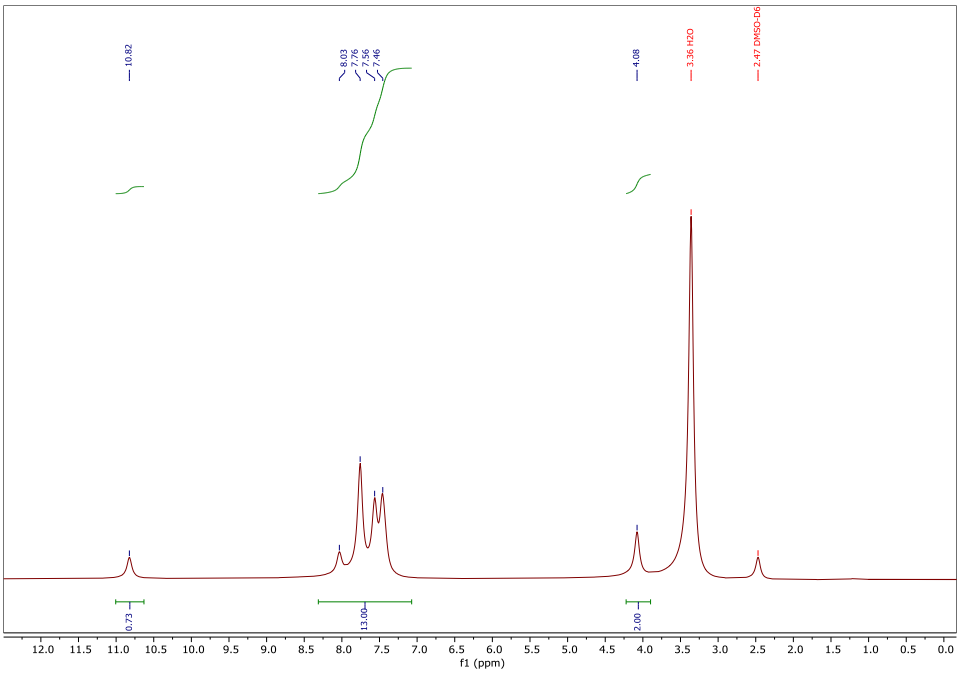

Figure S11. ^{1}H NMR spectrum (500 MHz, DMSO-d_6) for compound **3e**.

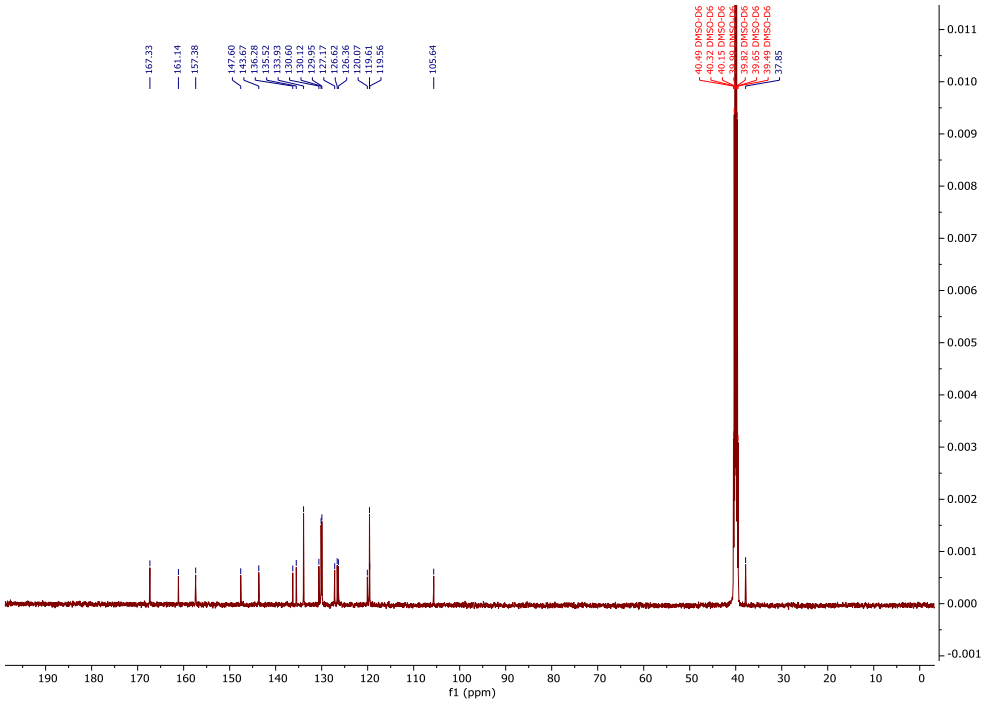

Figure S12. ^{13}C NMR spectrum (125 MHz, DMSO-d_6) for compound **3e**.

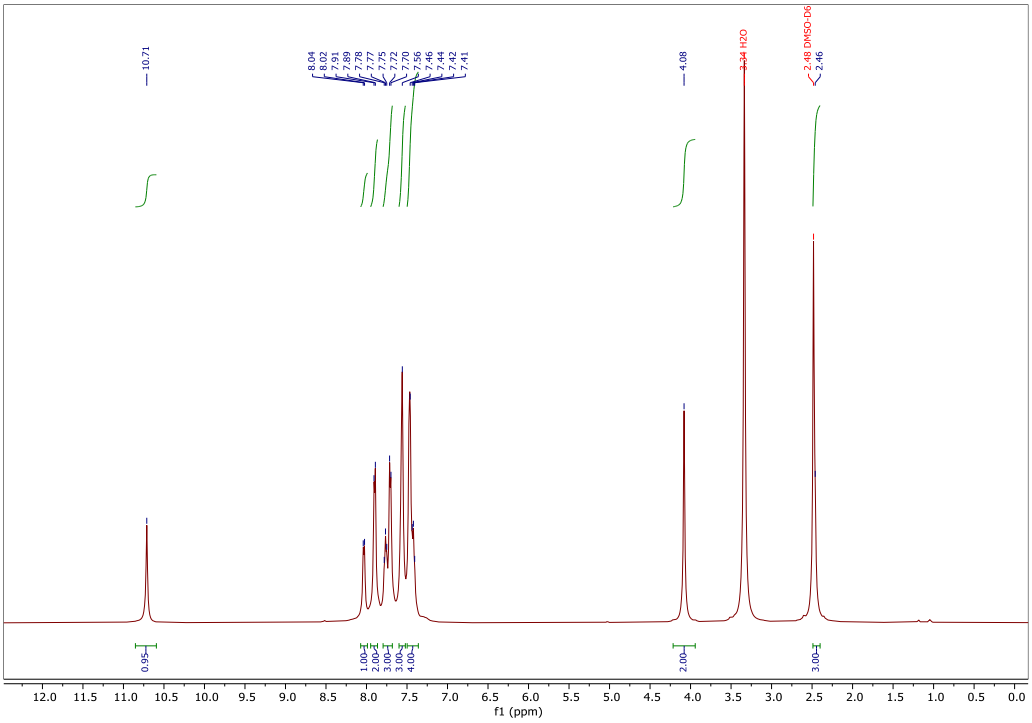

Figure S13. ^{1}H NMR spectrum (500 MHz, DMSO-d_6) for compound **3f**.

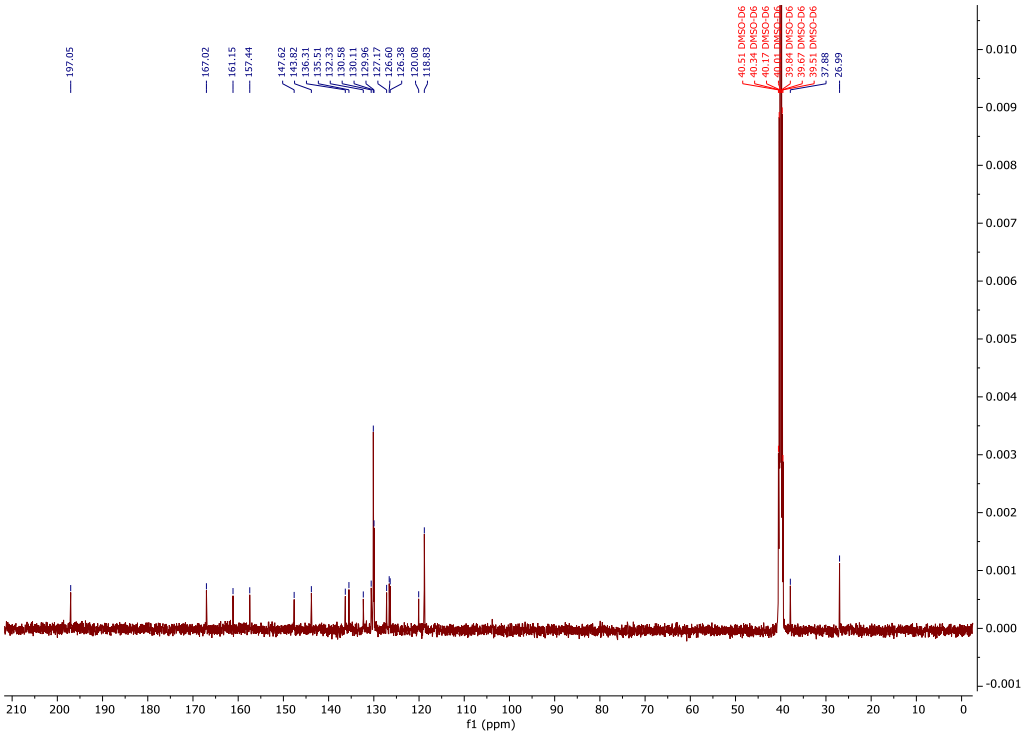

Figure S14. ^{13}C NMR spectrum (125 MHz, DMSO-d_6) for compound **3f**.

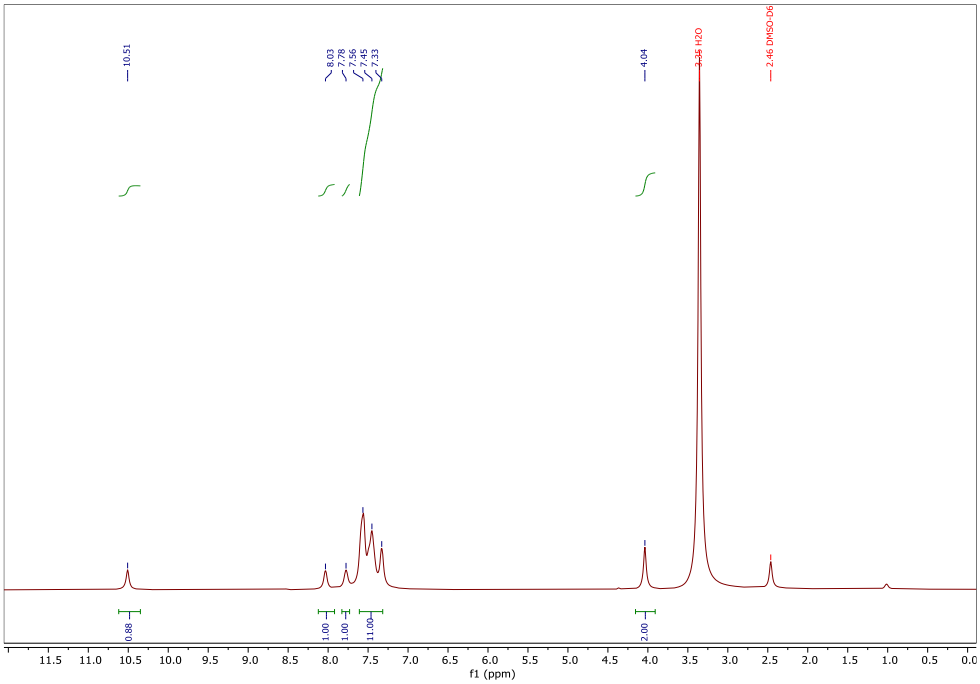

Figure S15. ^{1}H NMR spectrum (500 MHz, DMSO-d_6) for compound **3g**.

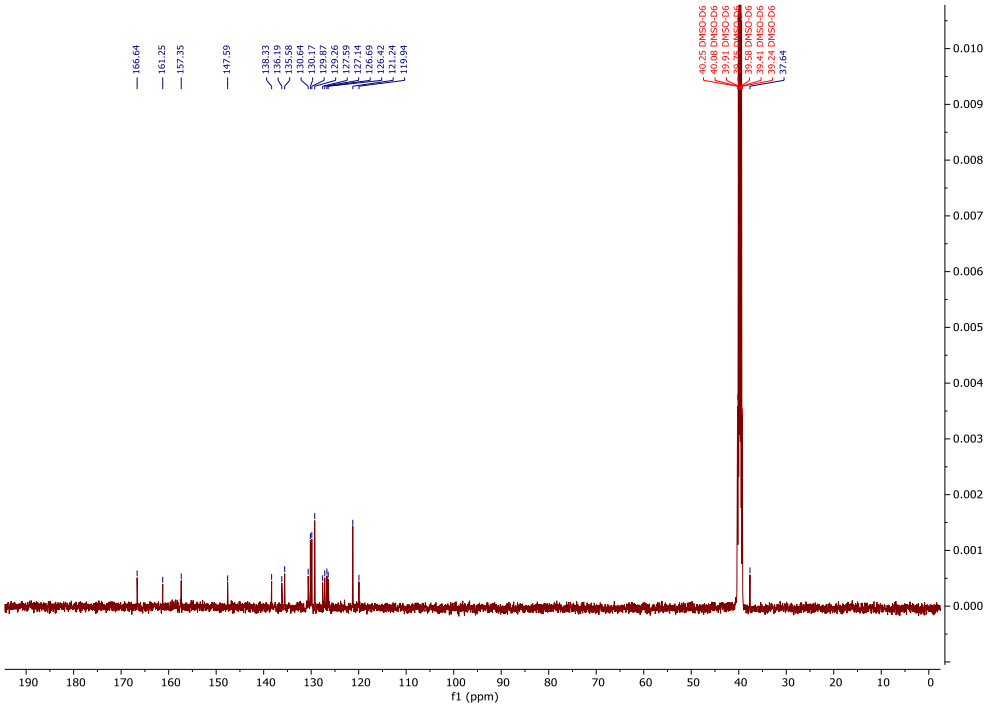

Figure S16. ^{13}C NMR spectrum (125 MHz, DMSO-d_6) for compound **3g**.

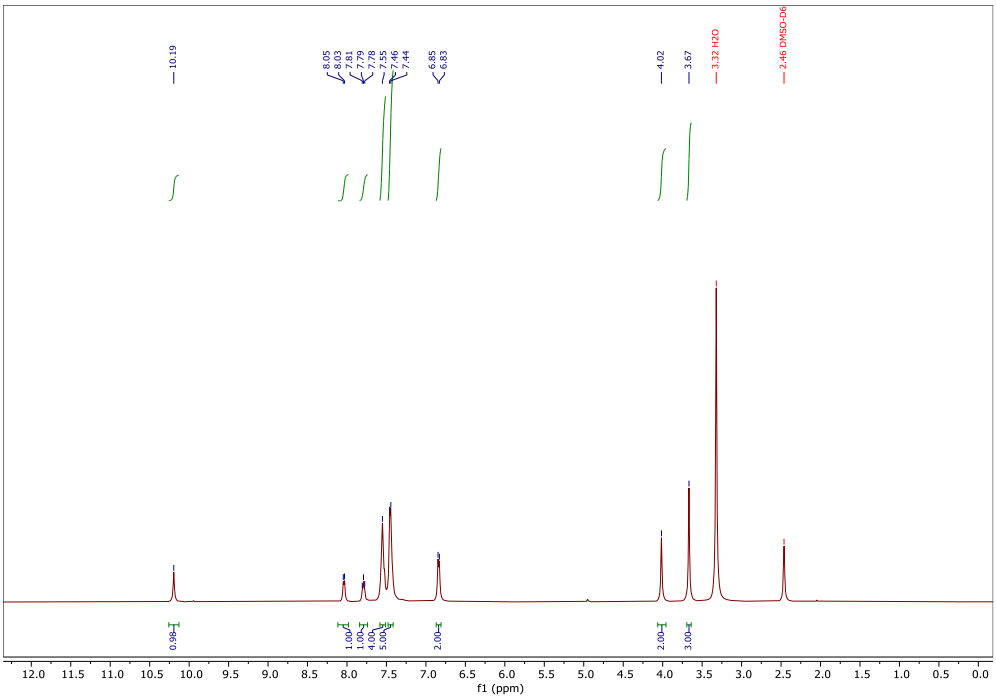

Figure S17. ^{1}H NMR spectrum (500 MHz, DMSO-d_6) for compound **3h**.

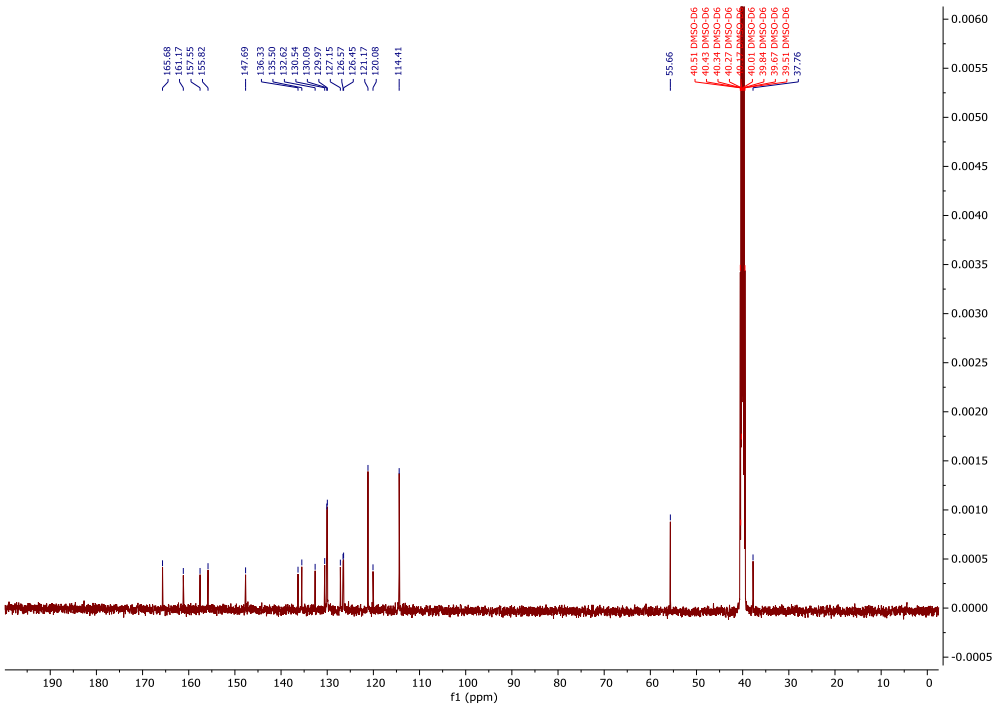

Figure S18. ^{13}C NMR spectrum (125 MHz, DMSO-d_6) for compound **3h**

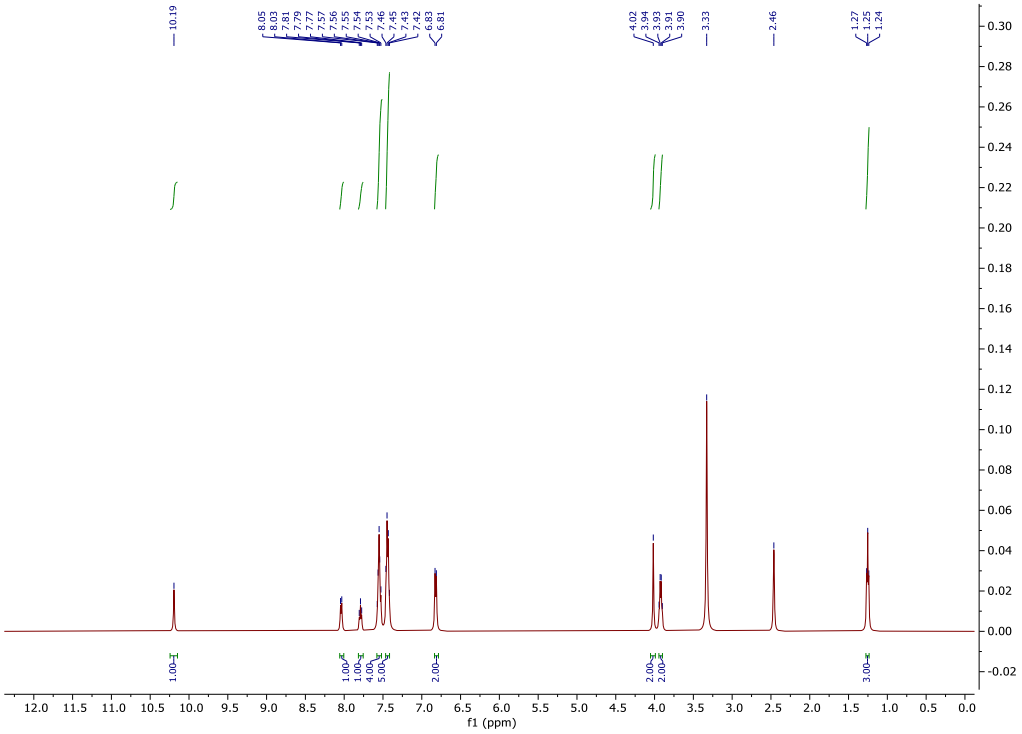

Figure S19. ^{1}H NMR spectrum (500 MHz, DMSO-d_6) for compound **3i**.

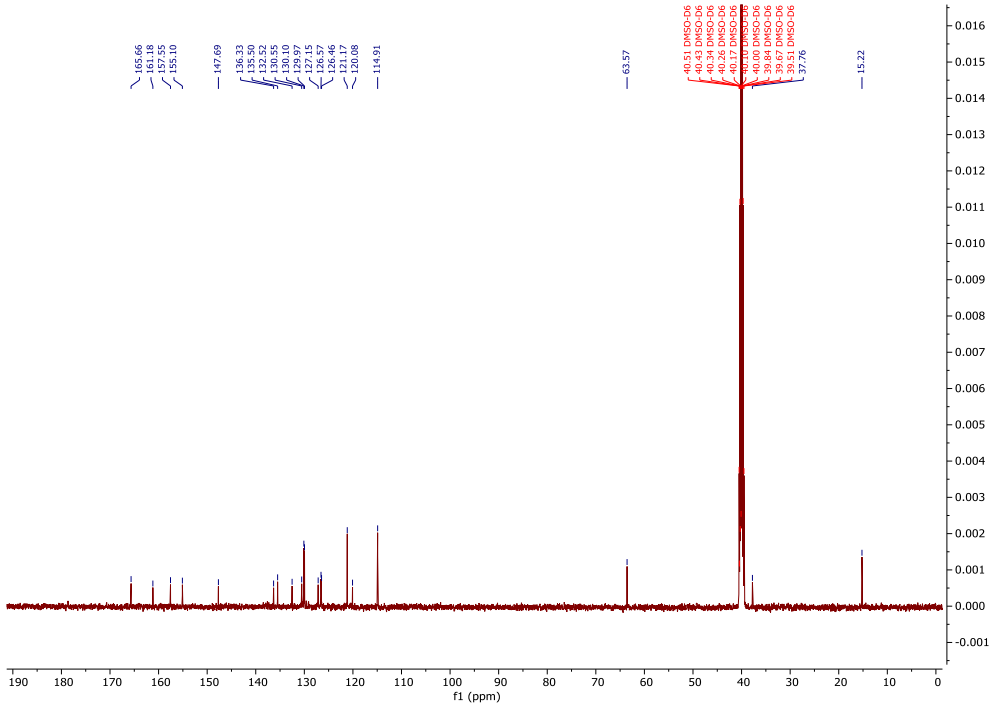

Figure S20. ^{13}C NMR spectrum (125 MHz, DMSO-d$_6$) for compound **3i**.

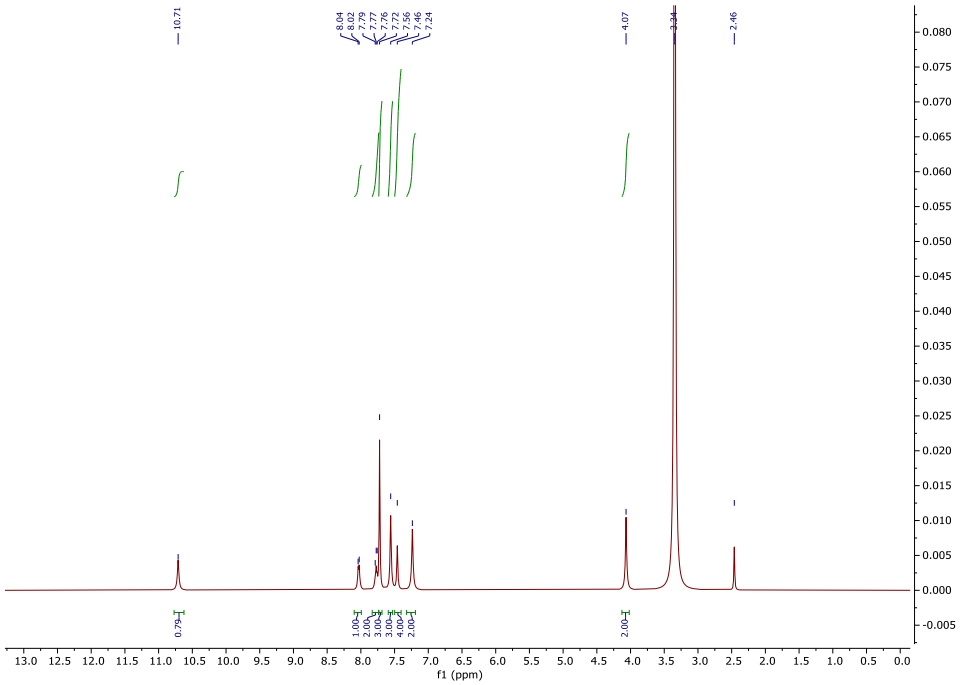

Figure S21. ^{1}H NMR spectrum (500 MHz, DMSO-d_6) for compound **3j**.

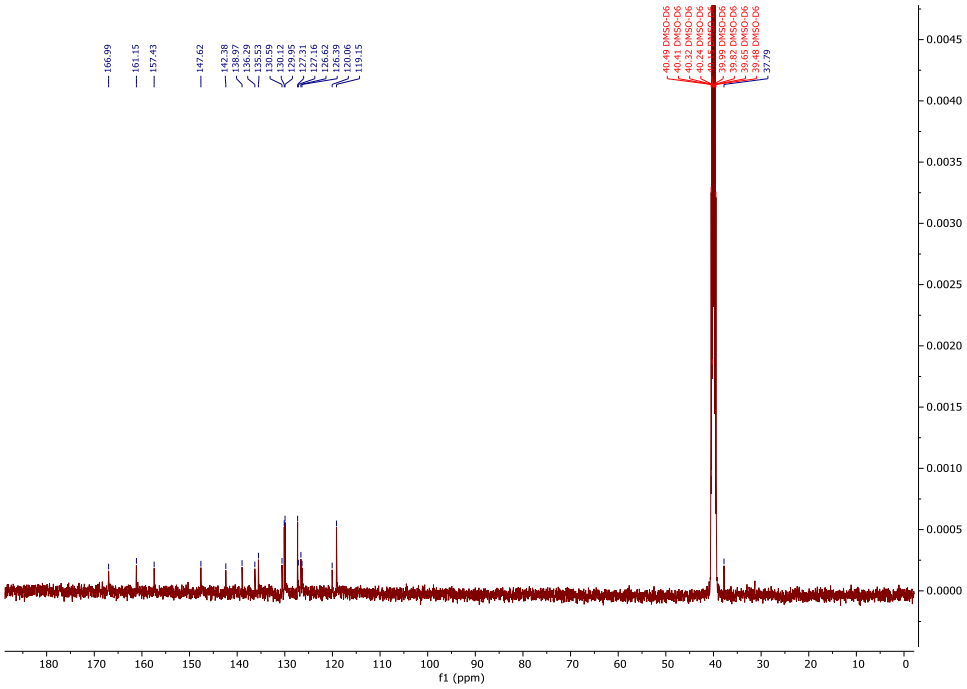

Figure S22. ^{13}C NMR spectrum (125 MHz, DMSO-d_6) for compound **3j**.

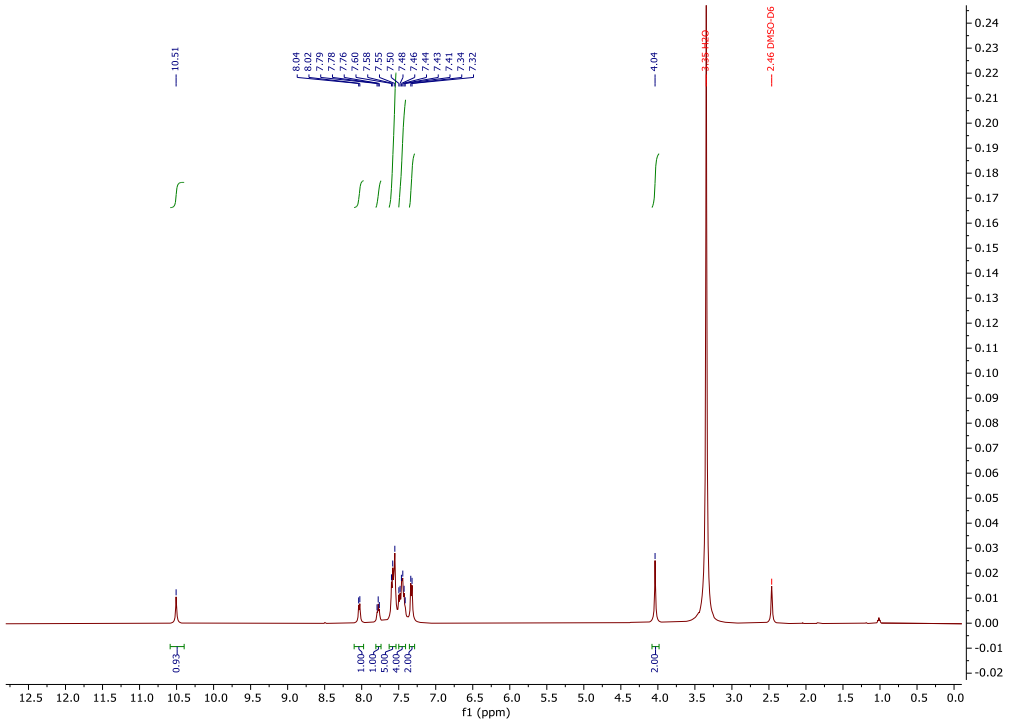

Figure S23. ^{1}H NMR spectrum (500 MHz, DMSO-d_6) for compound **3k**.

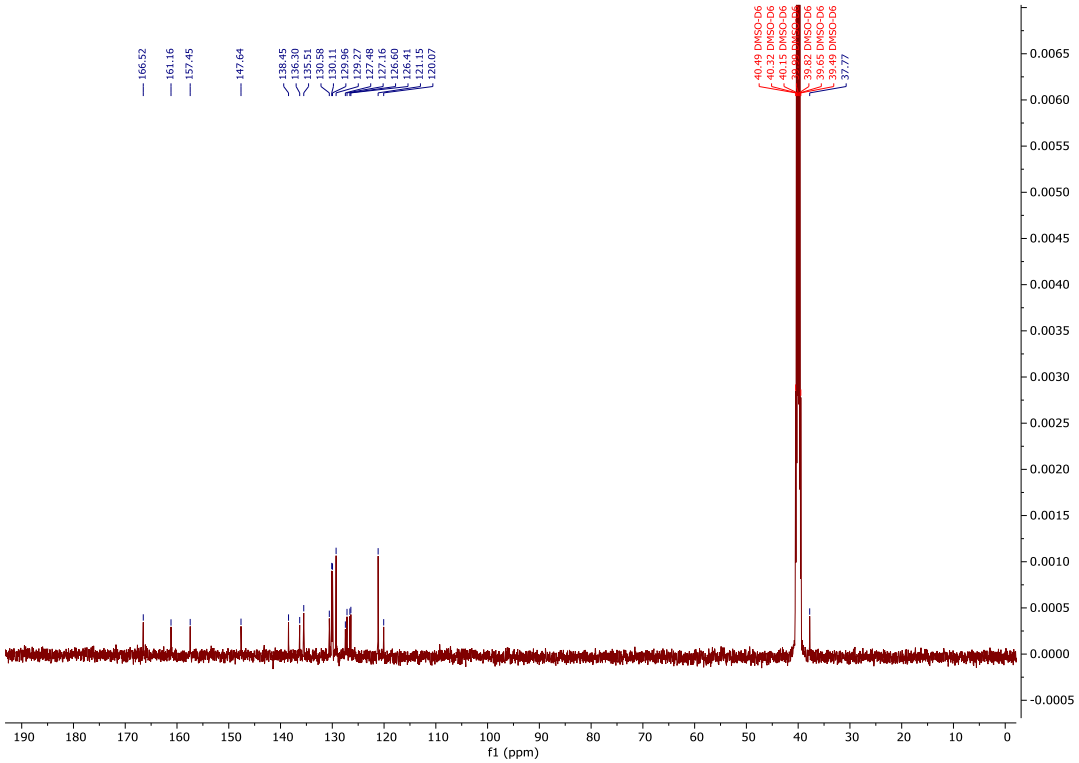

Figure S24. ^{13}C NMR spectrum (125 MHz, DMSO-d_6) for compound **3k**.

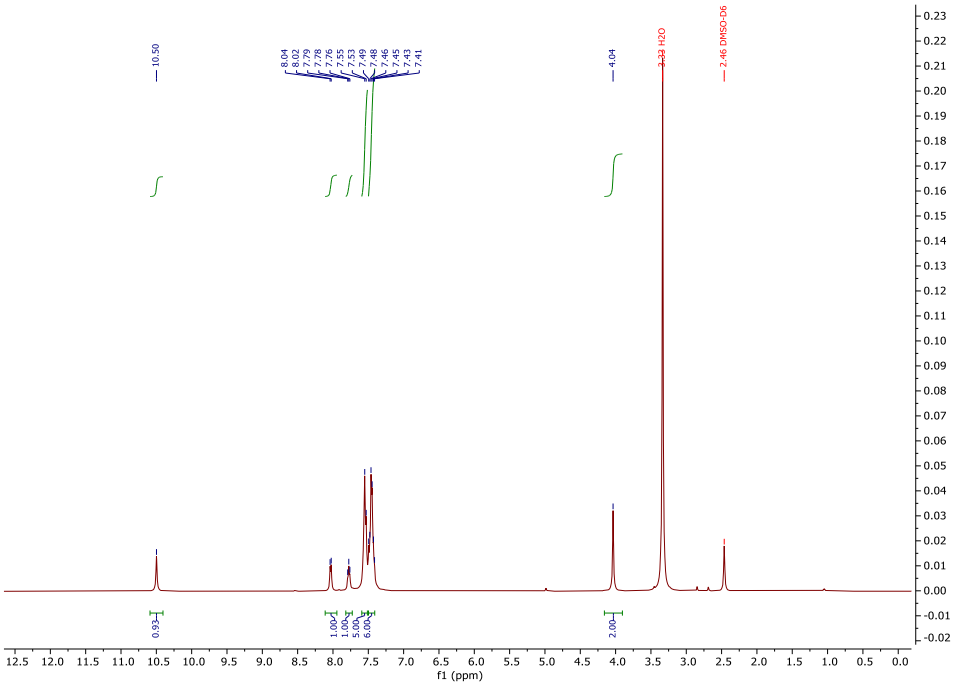

Figure S25. ^{1}H NMR spectrum (500 MHz, DMSO-d_6) for compound **3l**.

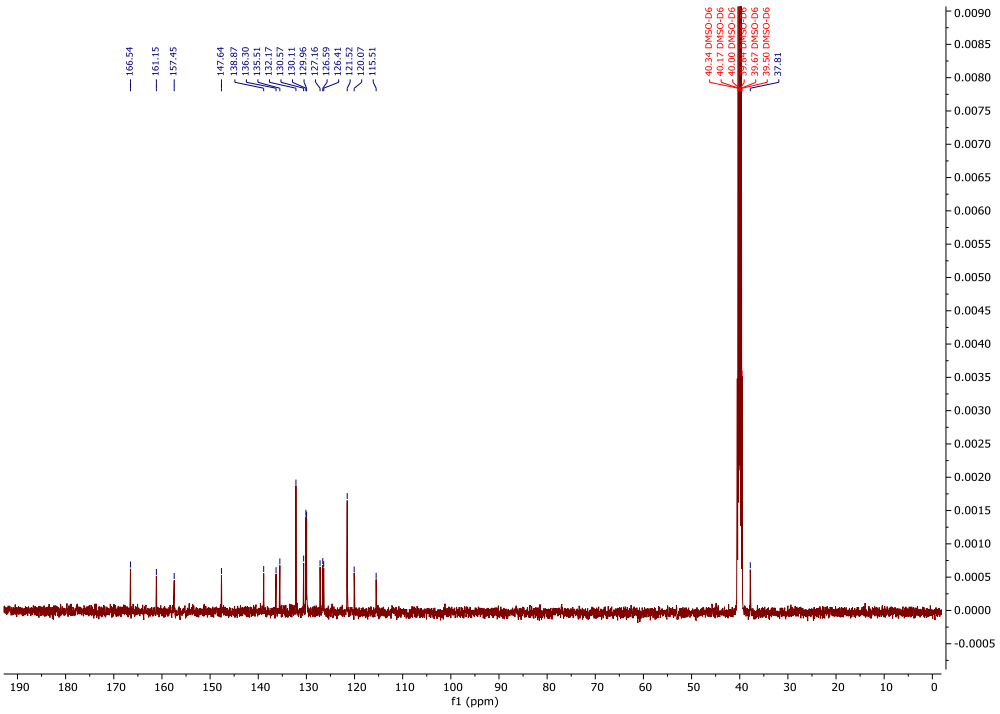

Figure S26. ^{13}C NMR spectrum (125 MHz, DMSO-d_6) for compound **3l**.

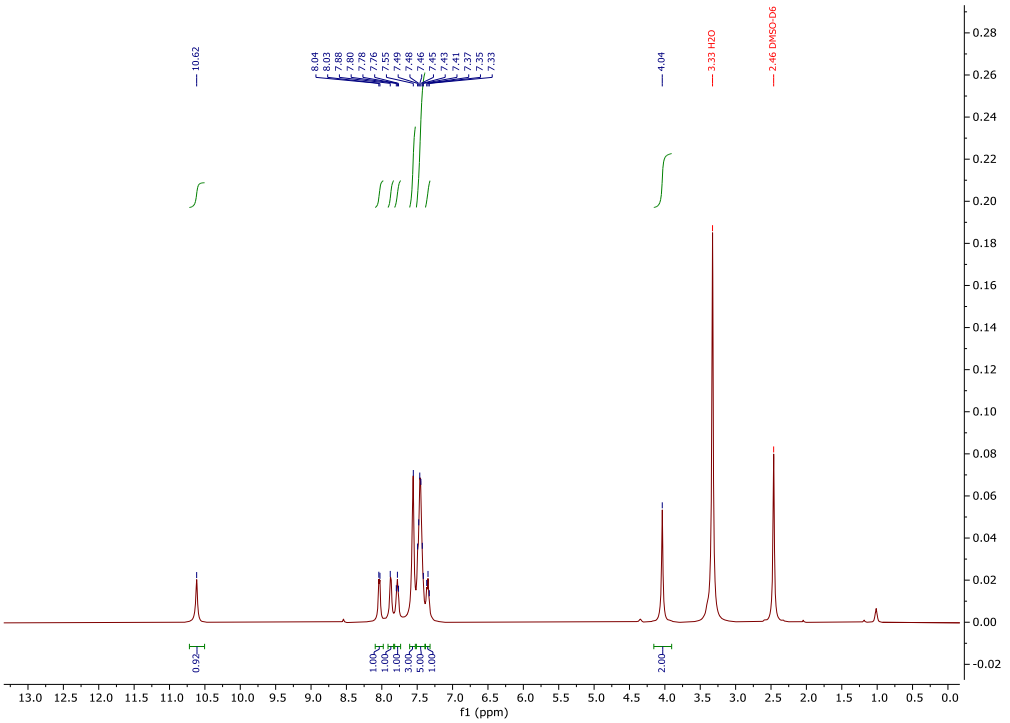

Figure S27. ^{1}H NMR spectrum (500 MHz, DMSO-d_6) for compound **3m**.

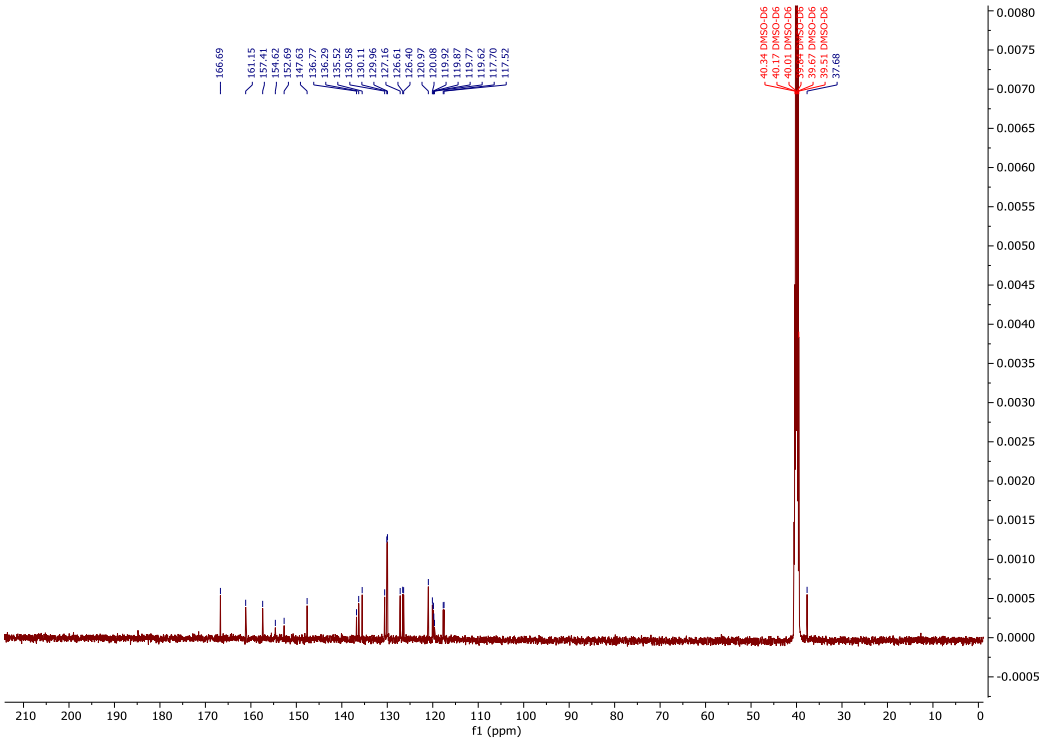

Figure S28. ^{13}C NMR spectrum (125 MHz, DMSO-d_6) for compound **3m**.

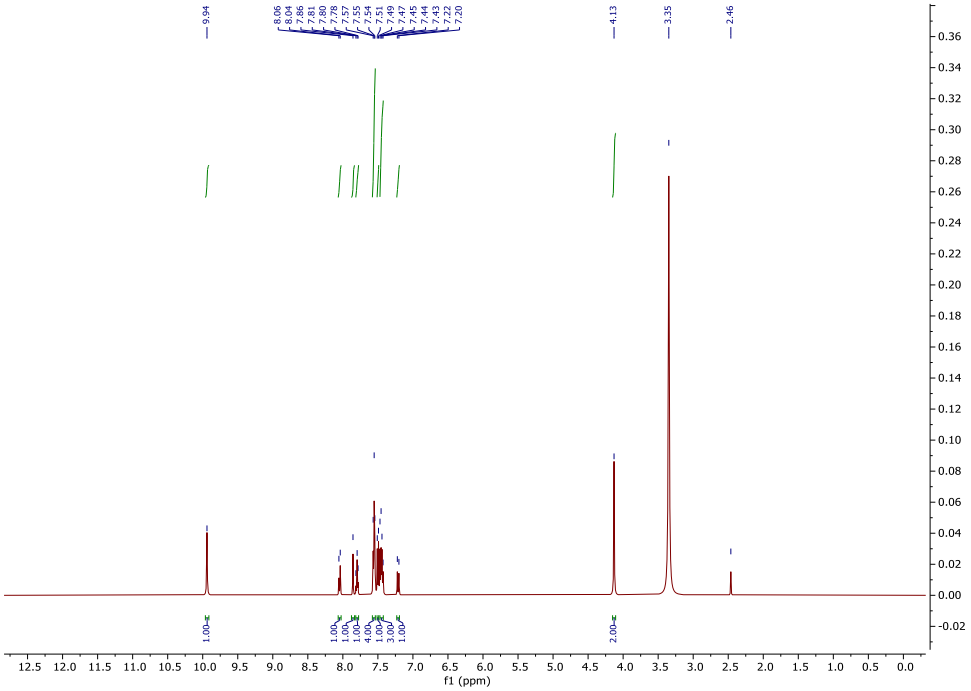

Figure S29. ^{1}H NMR spectrum (500 MHz, DMSO-d_6) for compound **3n**.

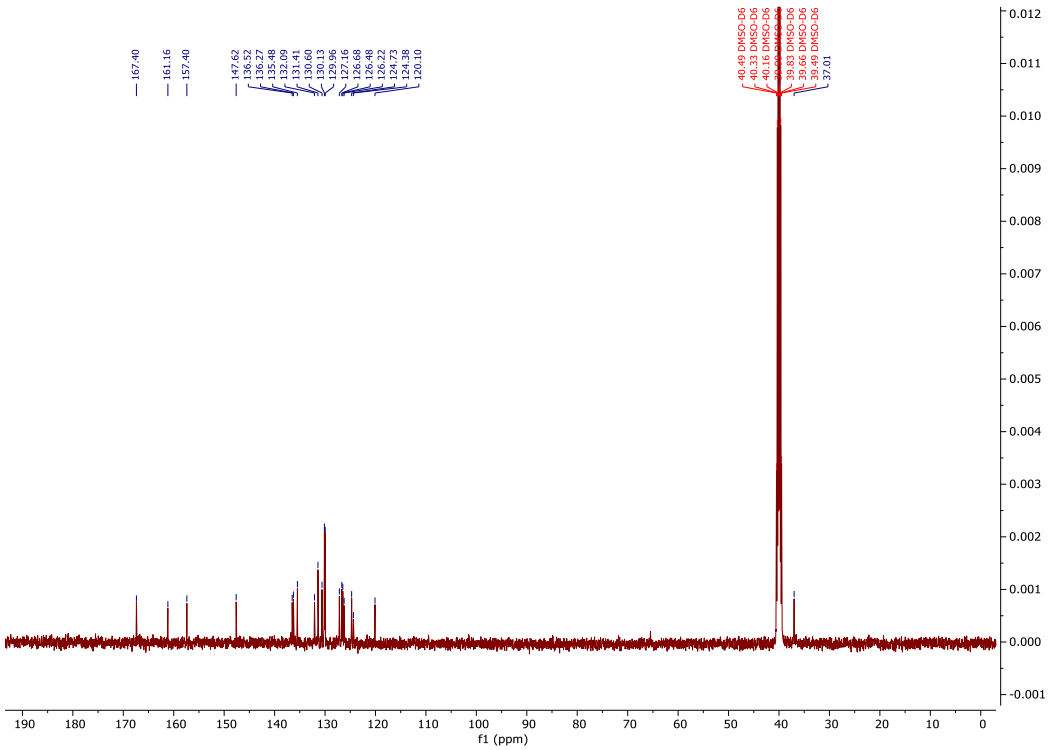

Figure S30. ^{13}C NMR spectrum (125 MHz, DMSO-d_6) for compound **3n**.

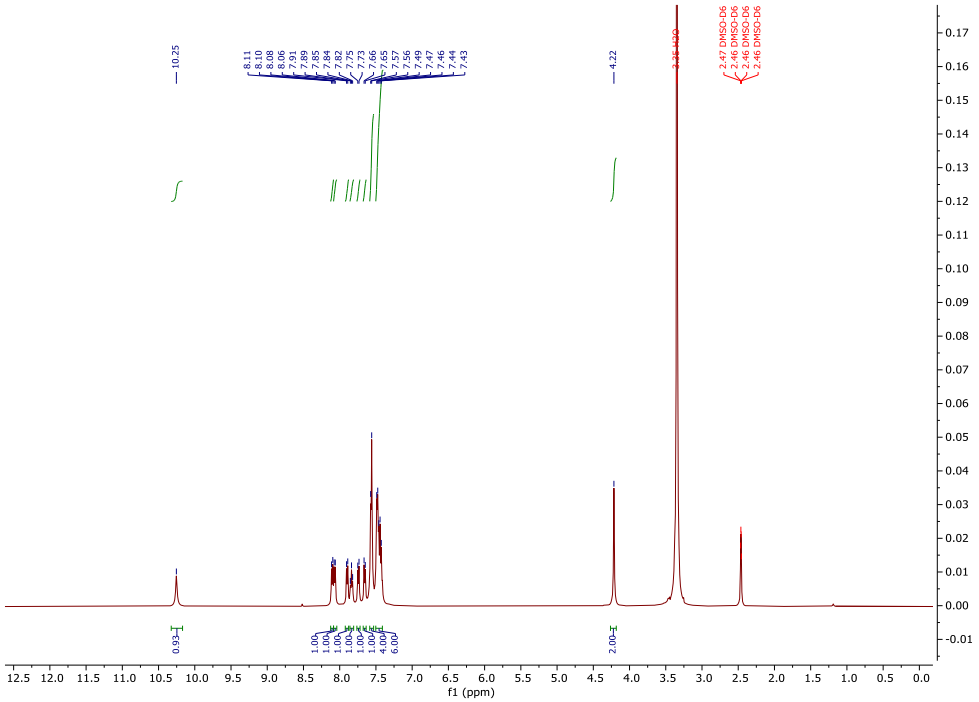

Figure S31. ^{1}H NMR spectrum (500 MHz, DMSO-d_6) for compound **3o**.

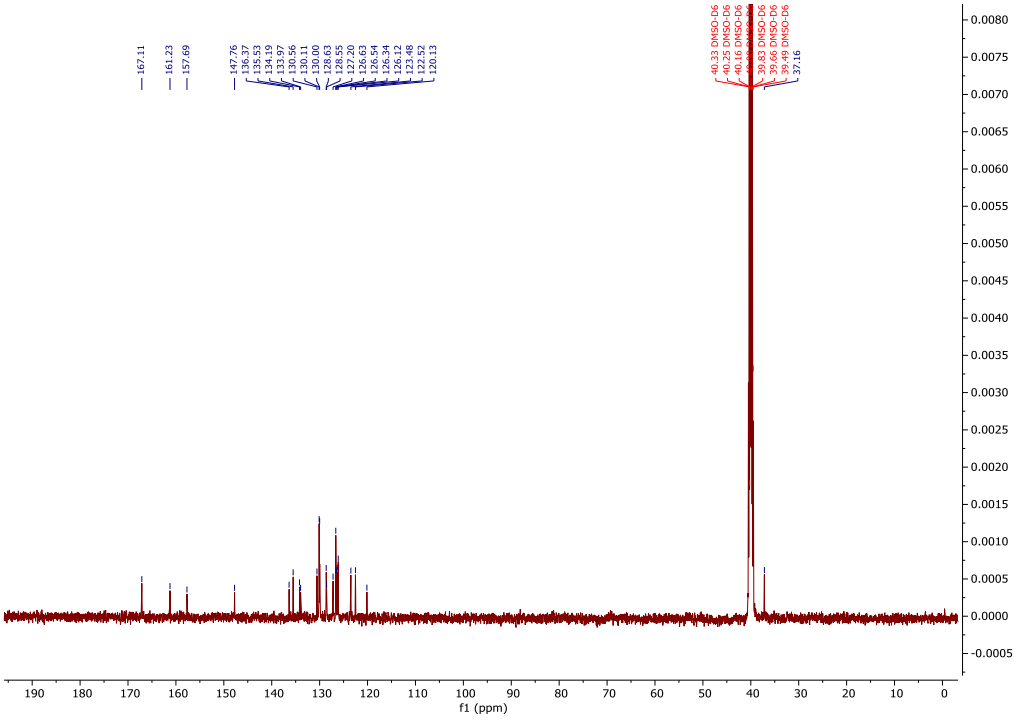

Figure S32. ^{13}C NMR spectrum (125 MHz, DMSO-d_6) for compound **3o**.

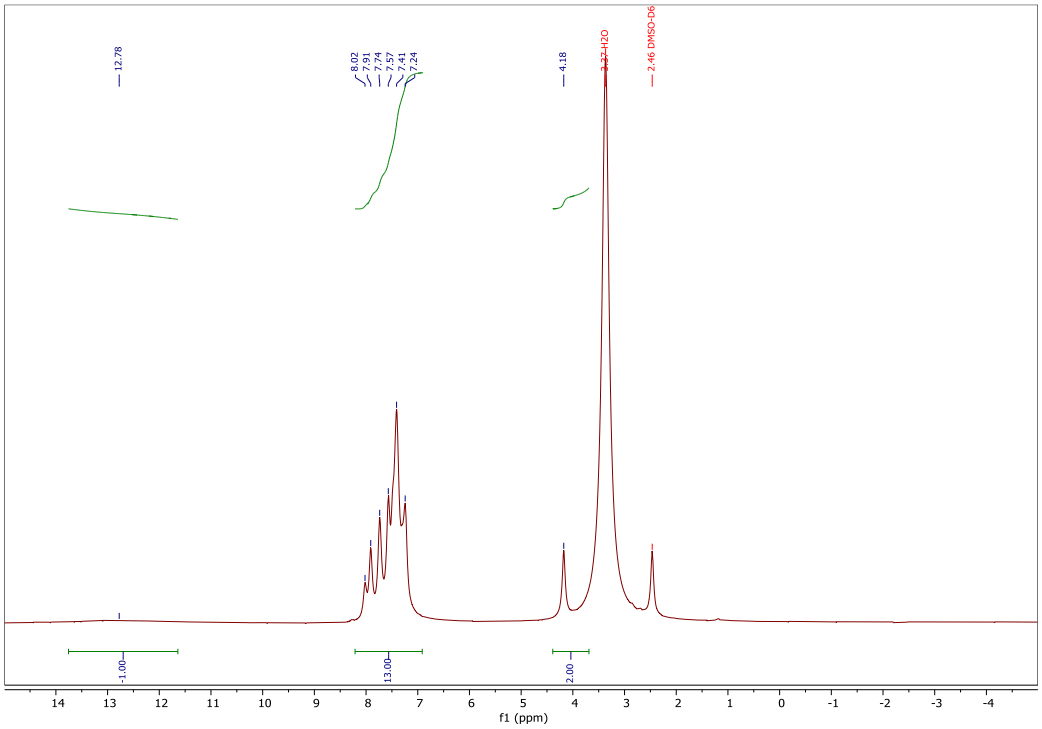

Figure S33. ^{1}H NMR spectrum (500 MHz, DMSO-d_6) for compound **3p**.

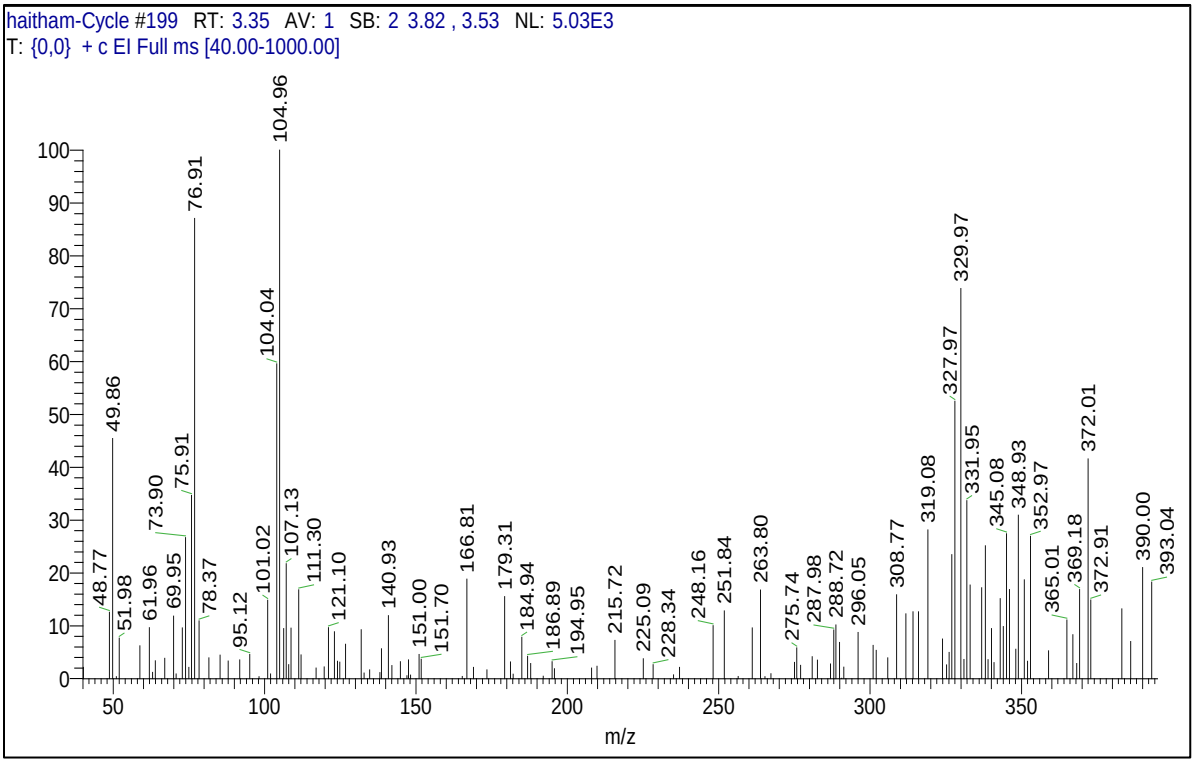

Figure S34. Mass spectrum for compound **3a**

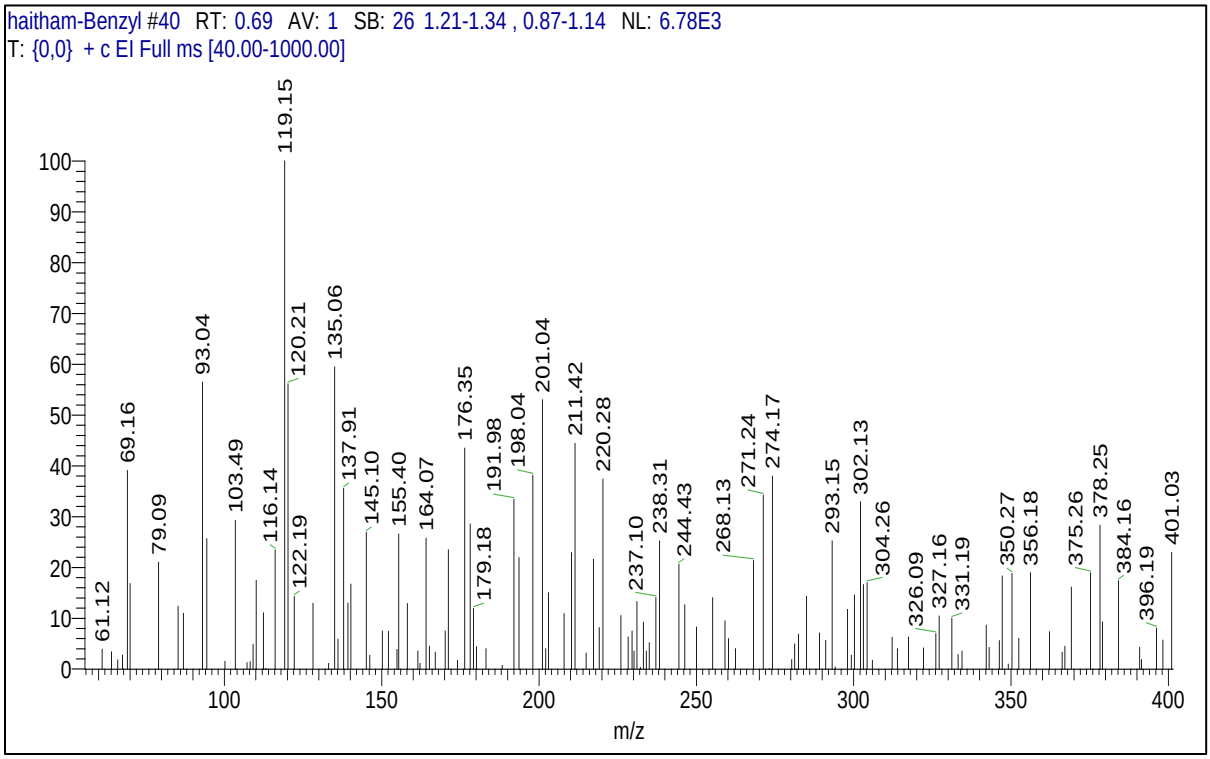

Figure S35. Mass spectrum for compound **3b.**

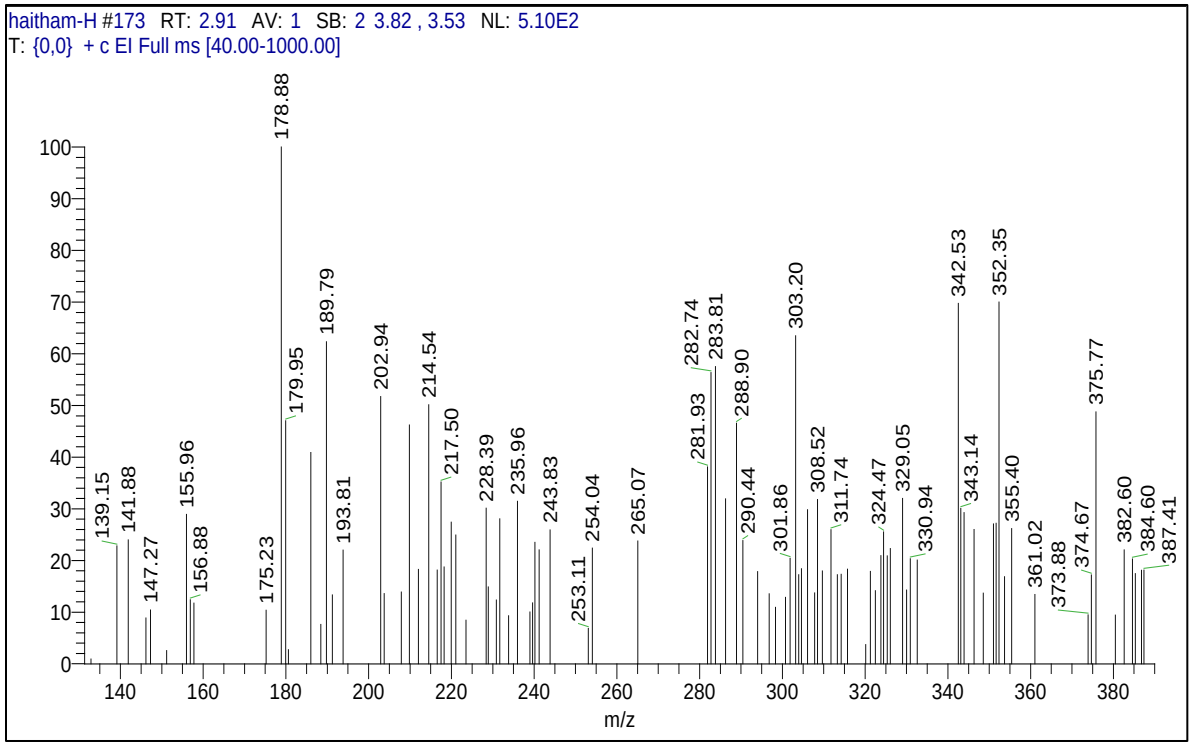

Figure S36. Mass spectrum for compound **3c.**

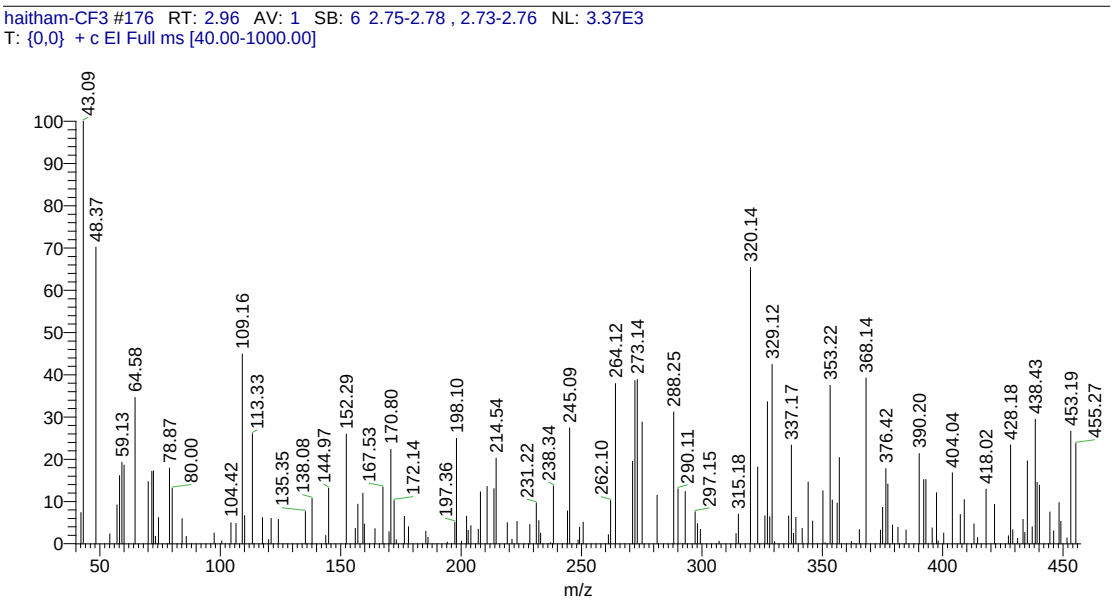

Figure S37. Mass spectrum for compound **3d.**

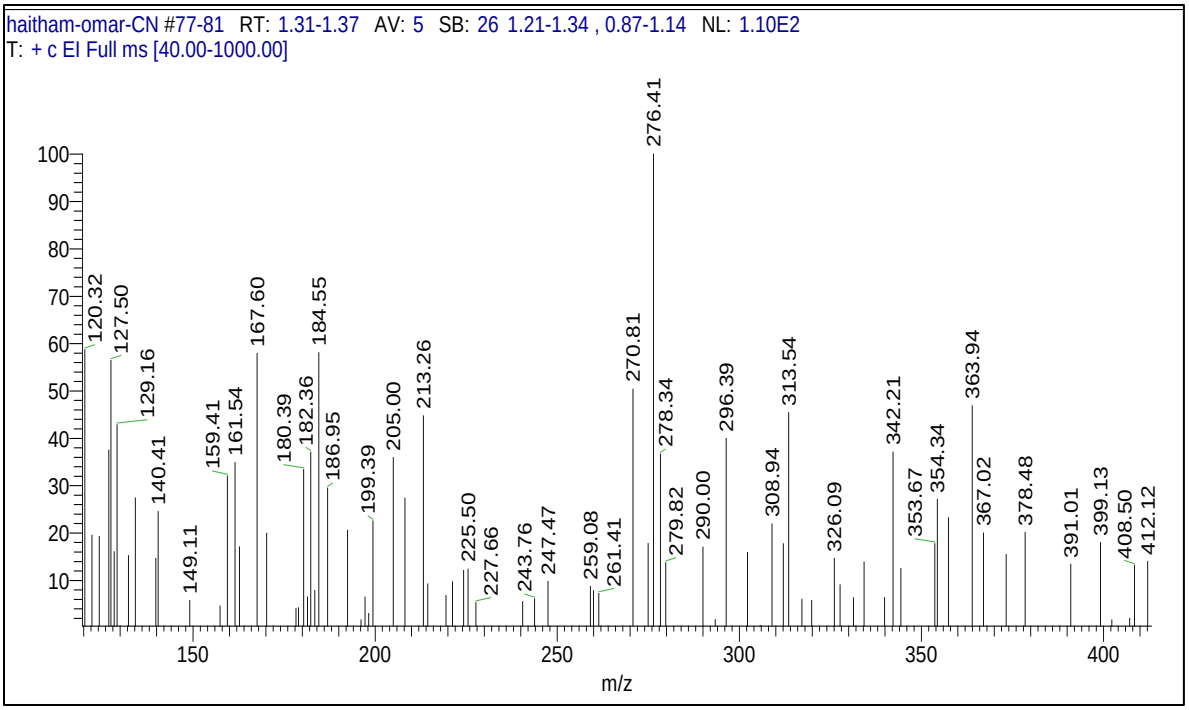

Figure S38. Mass spectrum for compound **3e.**

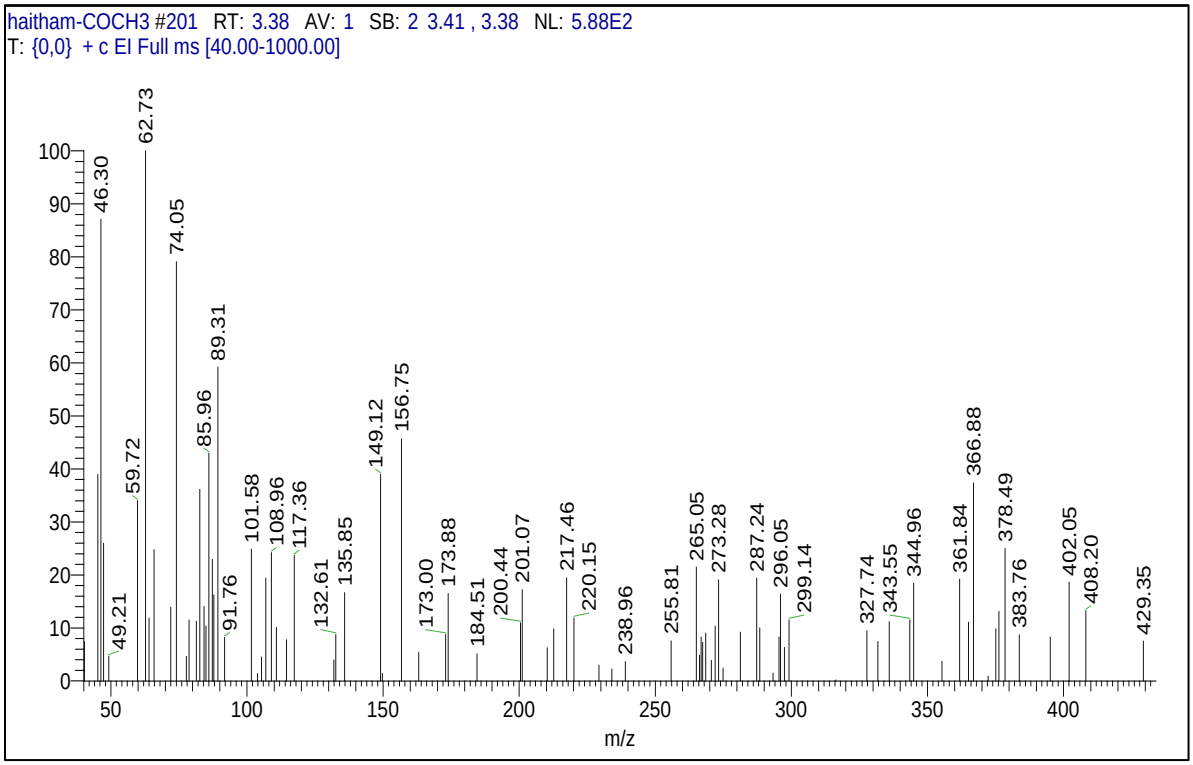

Figure S39. Mass spectrum for compound **3f.**

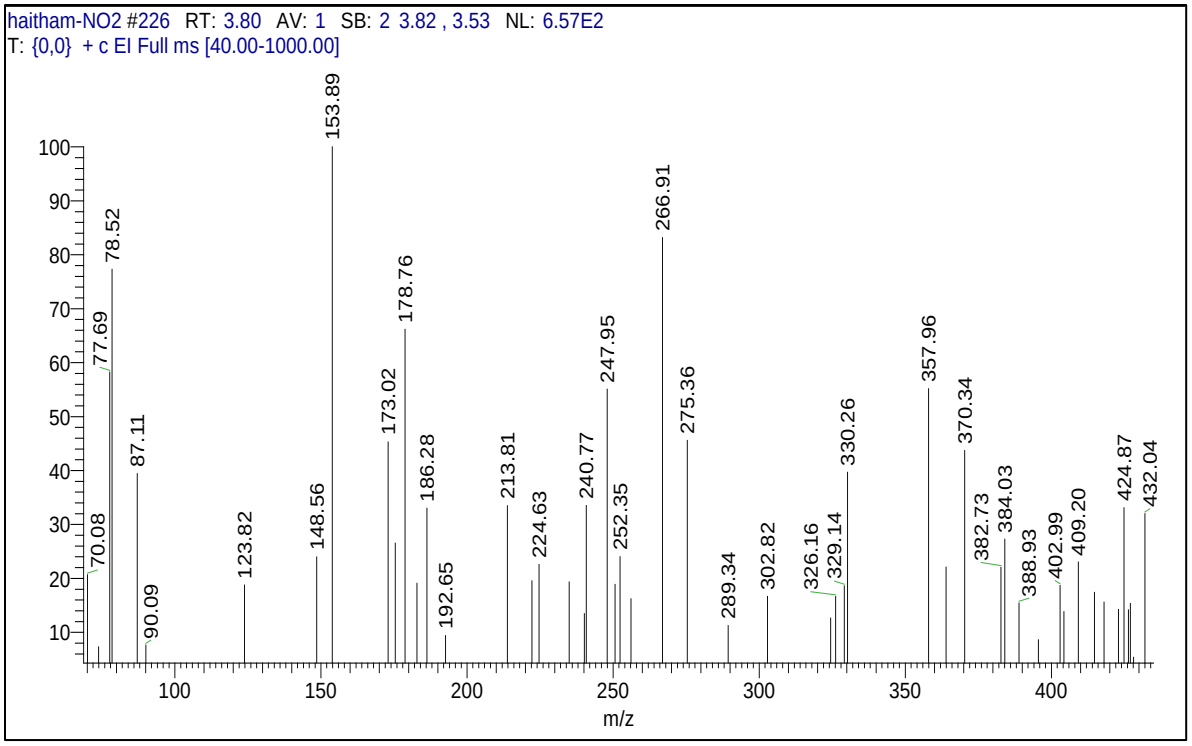

Figure S40. Mass spectrum for compound **3g.**

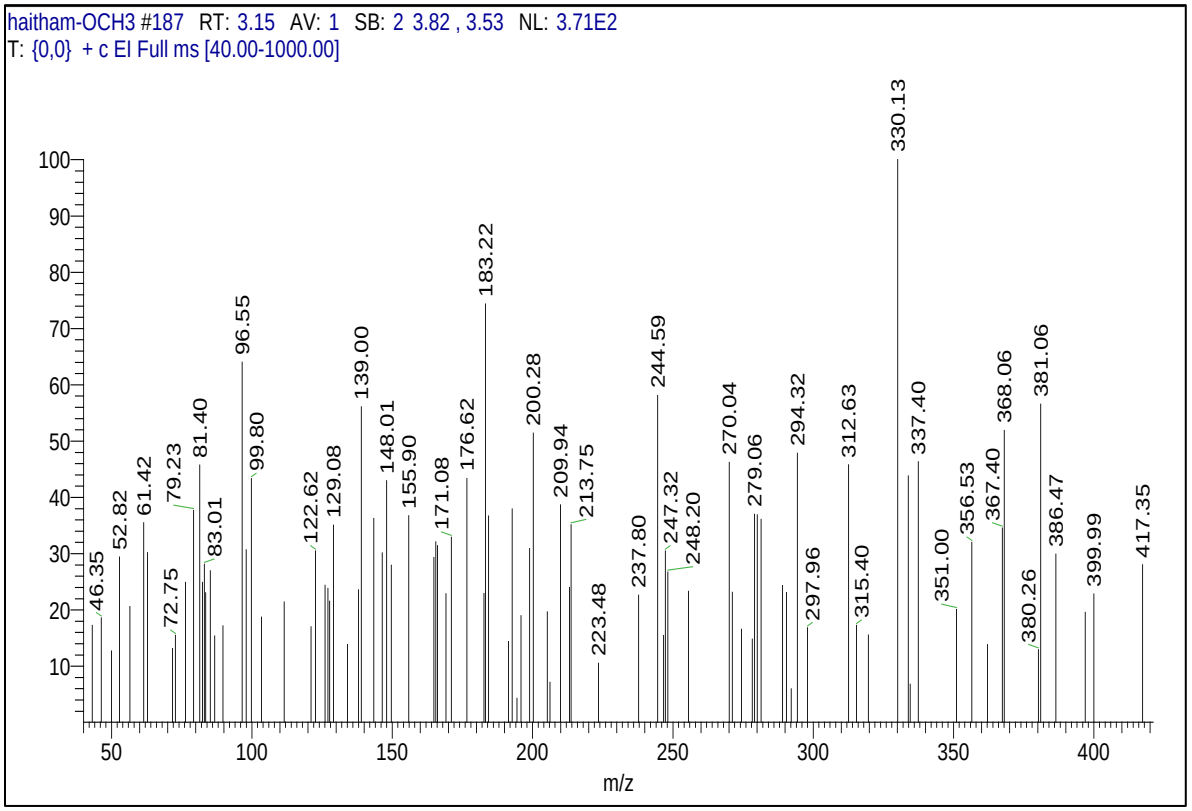

Figure S41. Mass spectrum for compound **3h.**

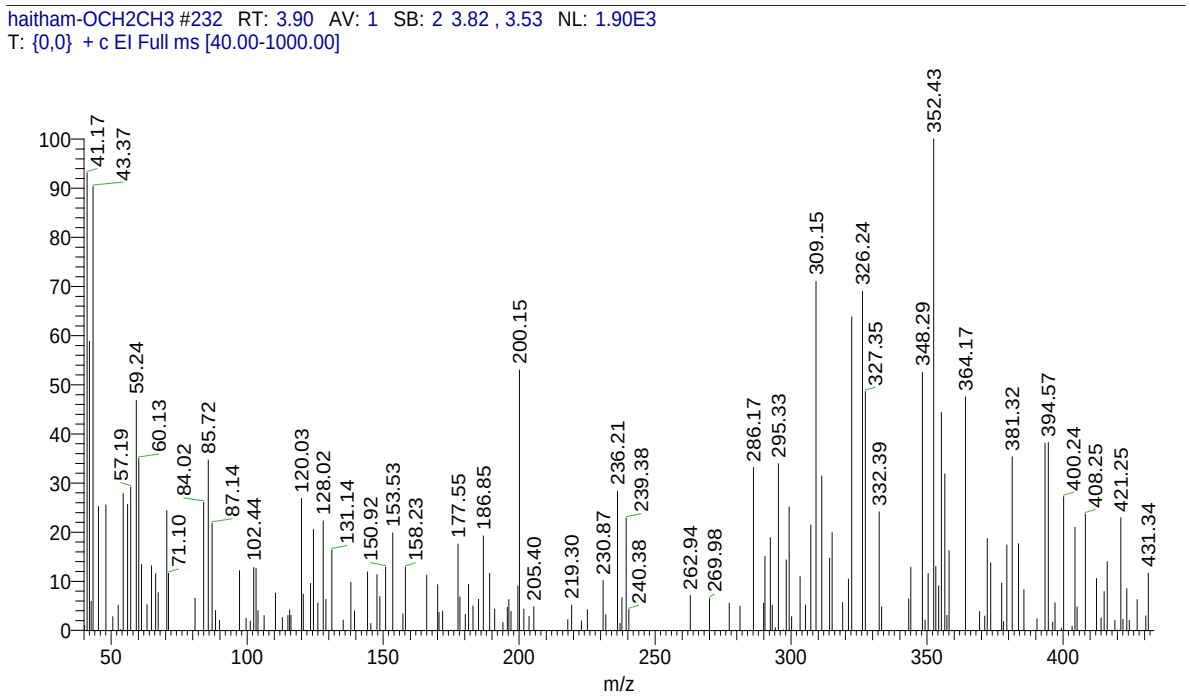

Figure S42. Mass spectrum for compound **3i.**

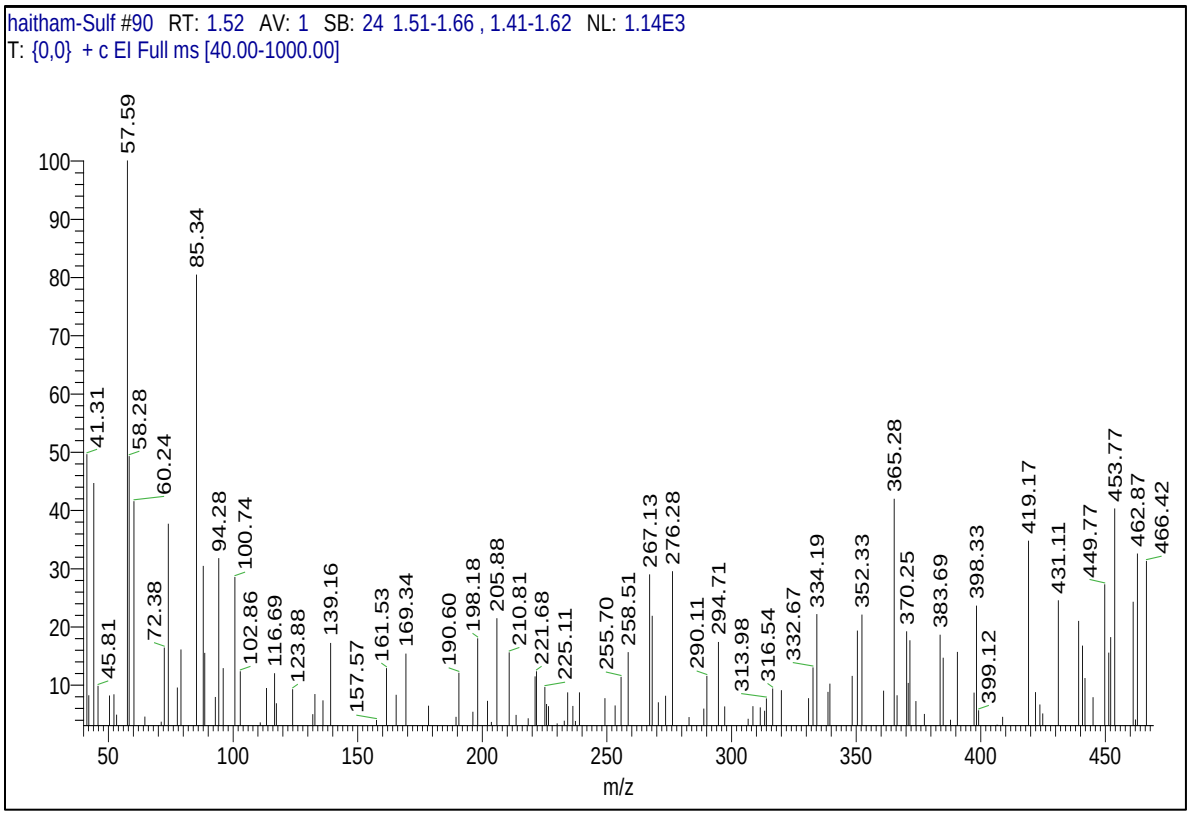

Figure S43. Mass spectrum for compound **3j.**

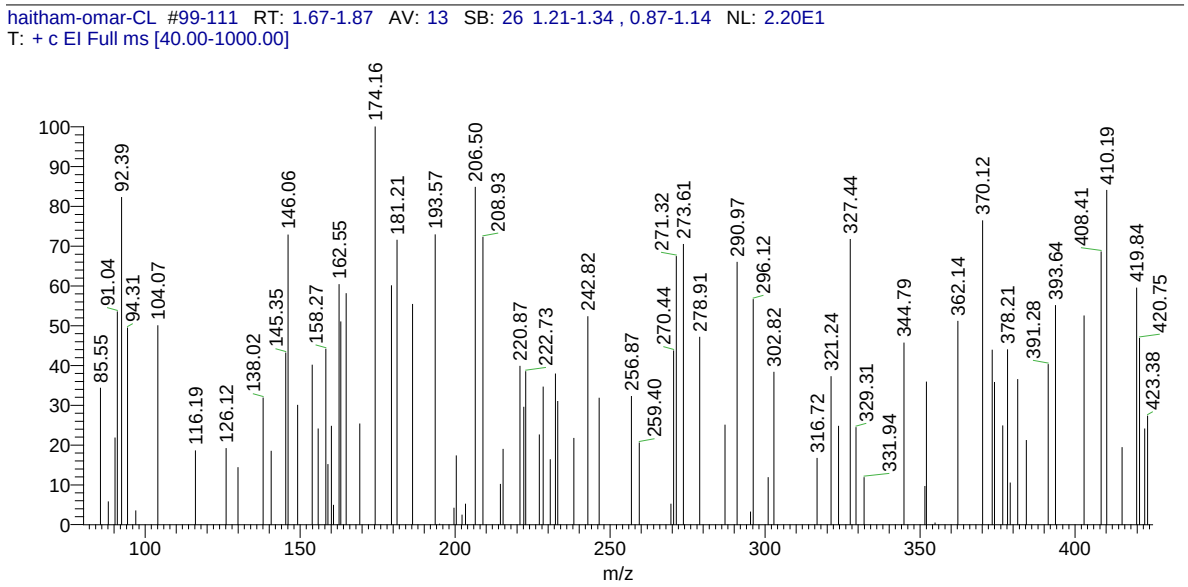

Figure S44. Mass spectrum for compound **3k.**

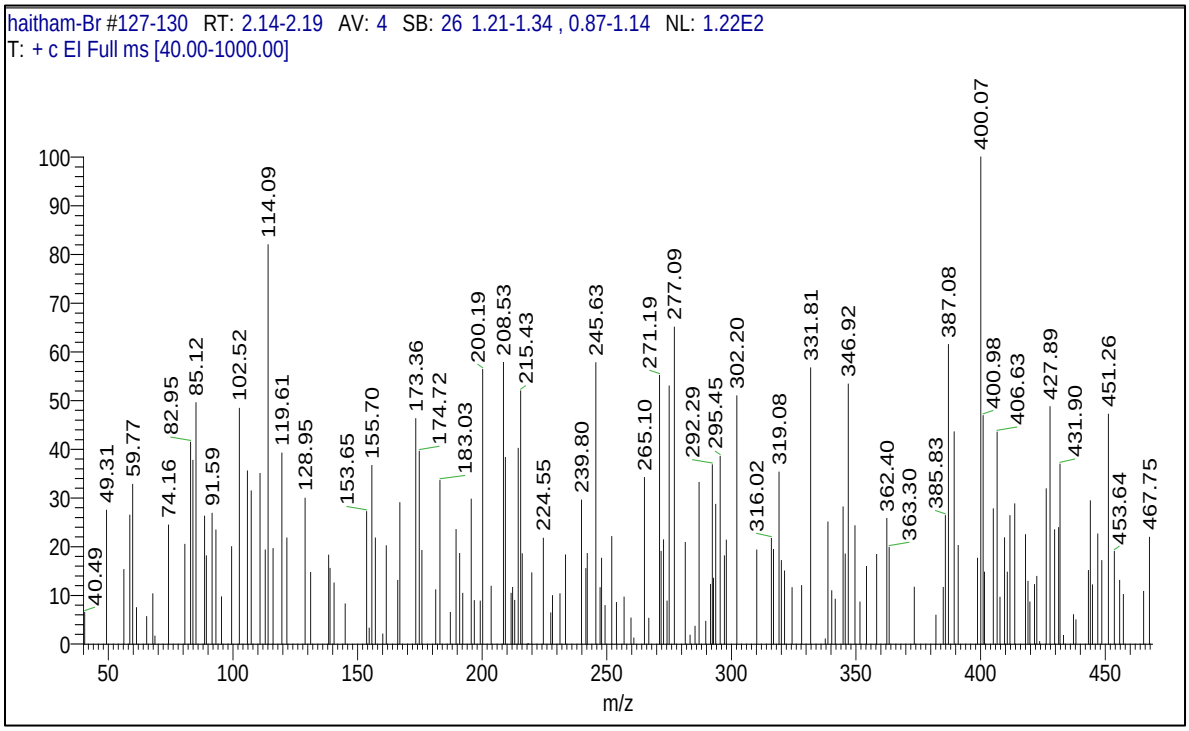

Figure S45. Mass spectrum for compound **3l.**

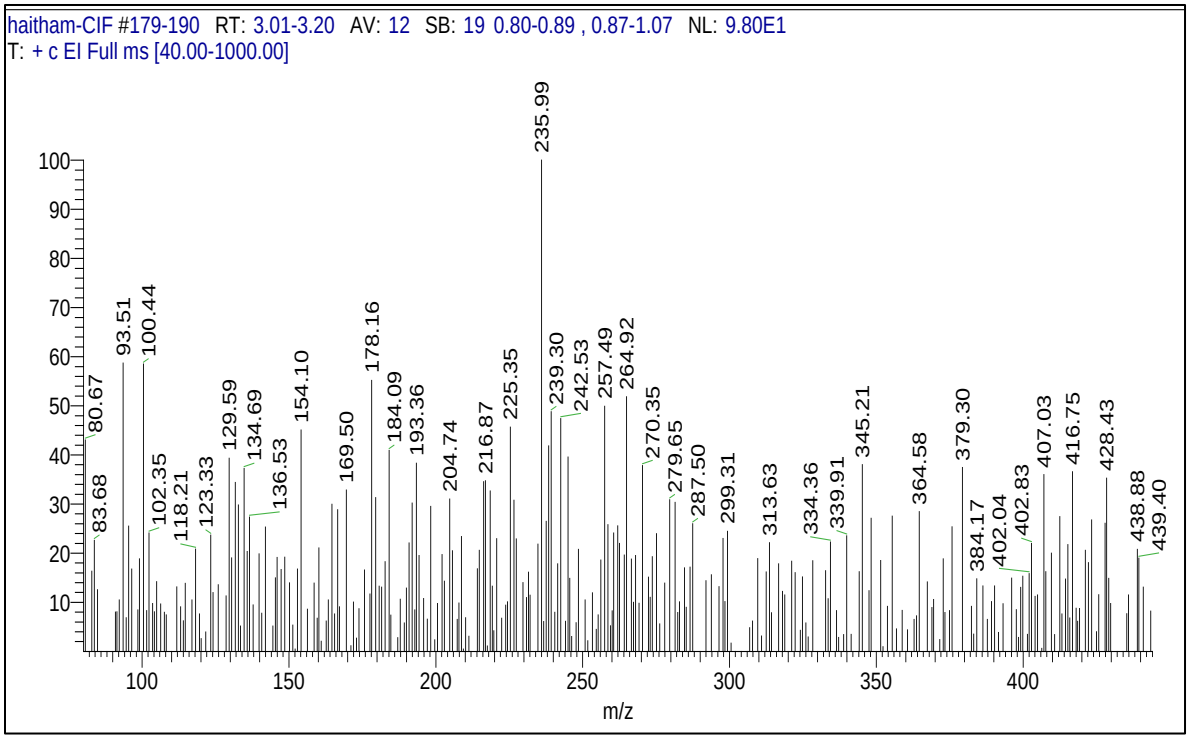

Figure S46. Mass spectrum for compound **3m.**

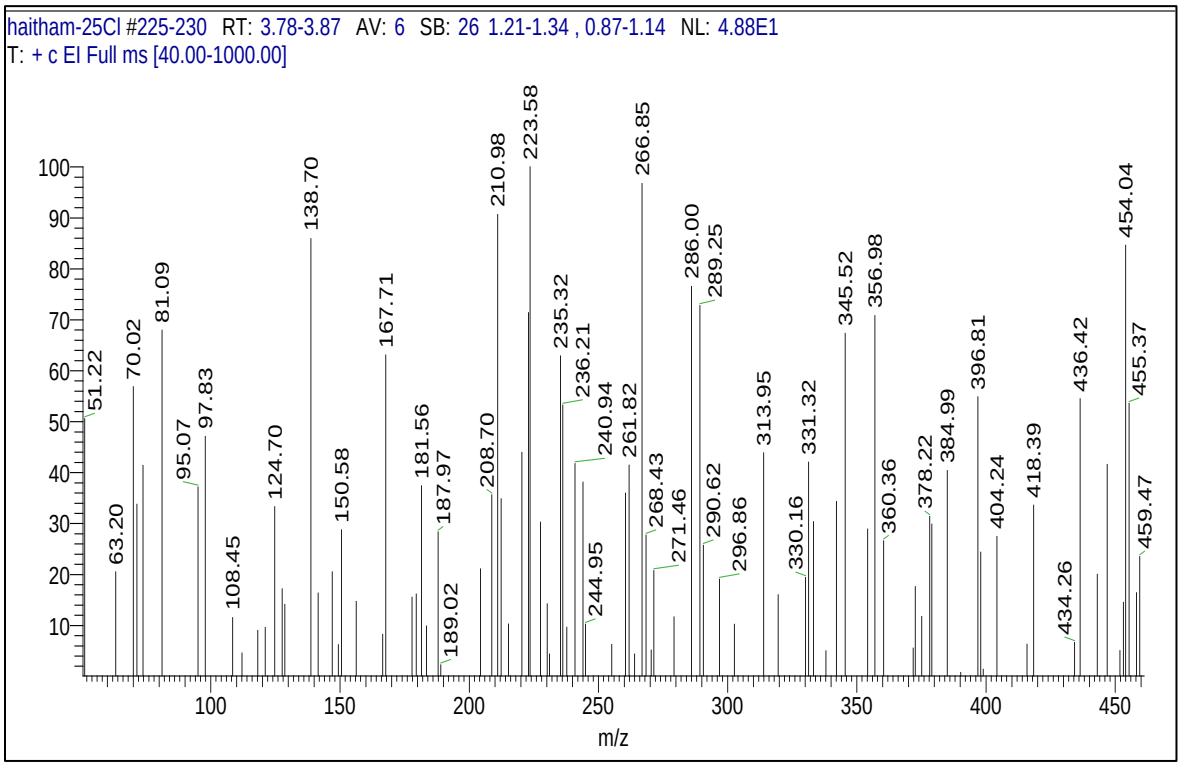

Figure S47. Mass spectrum for compound **3n.**

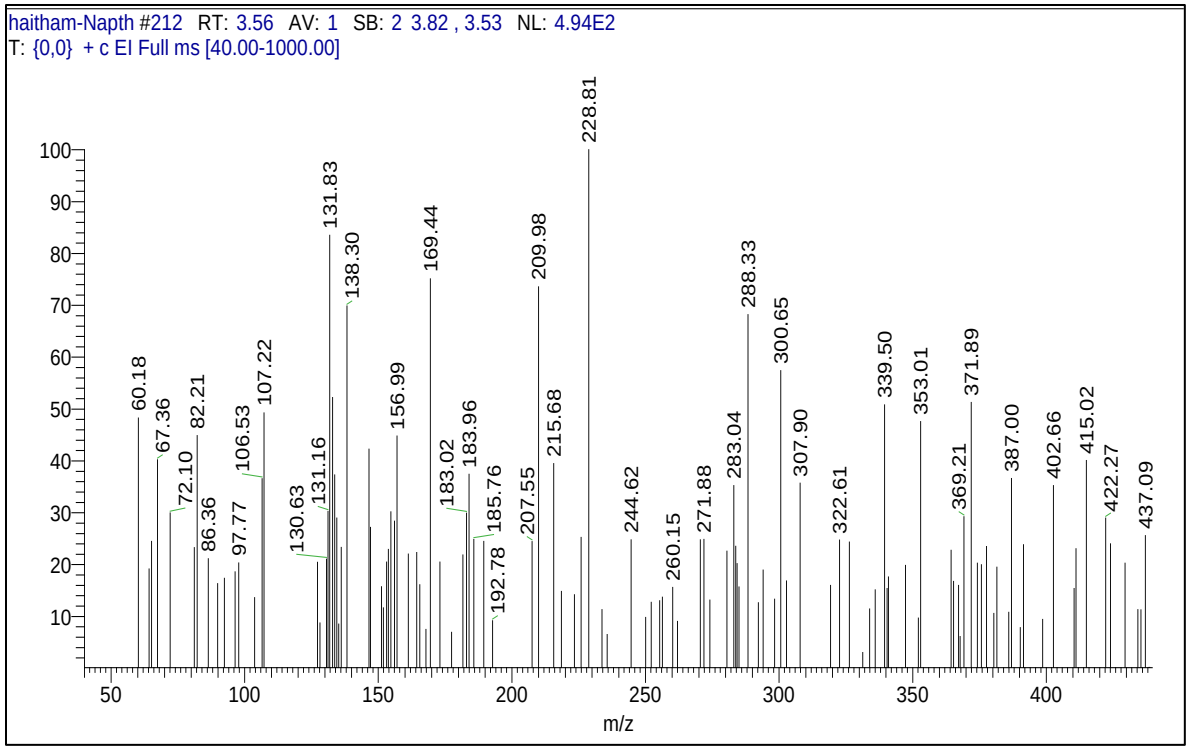

Figure S48. Mass spectrum for compound **3o.**

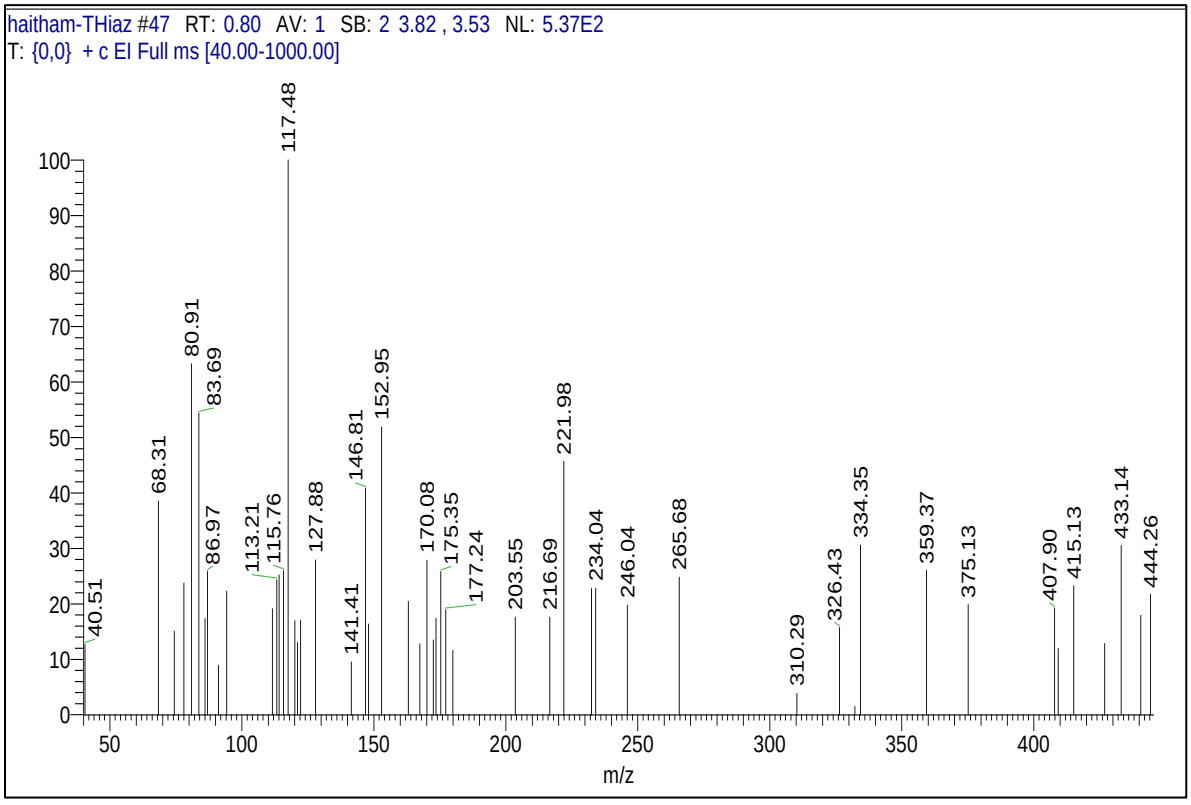

Figure S49. Mass spectrum for compound **3p.**

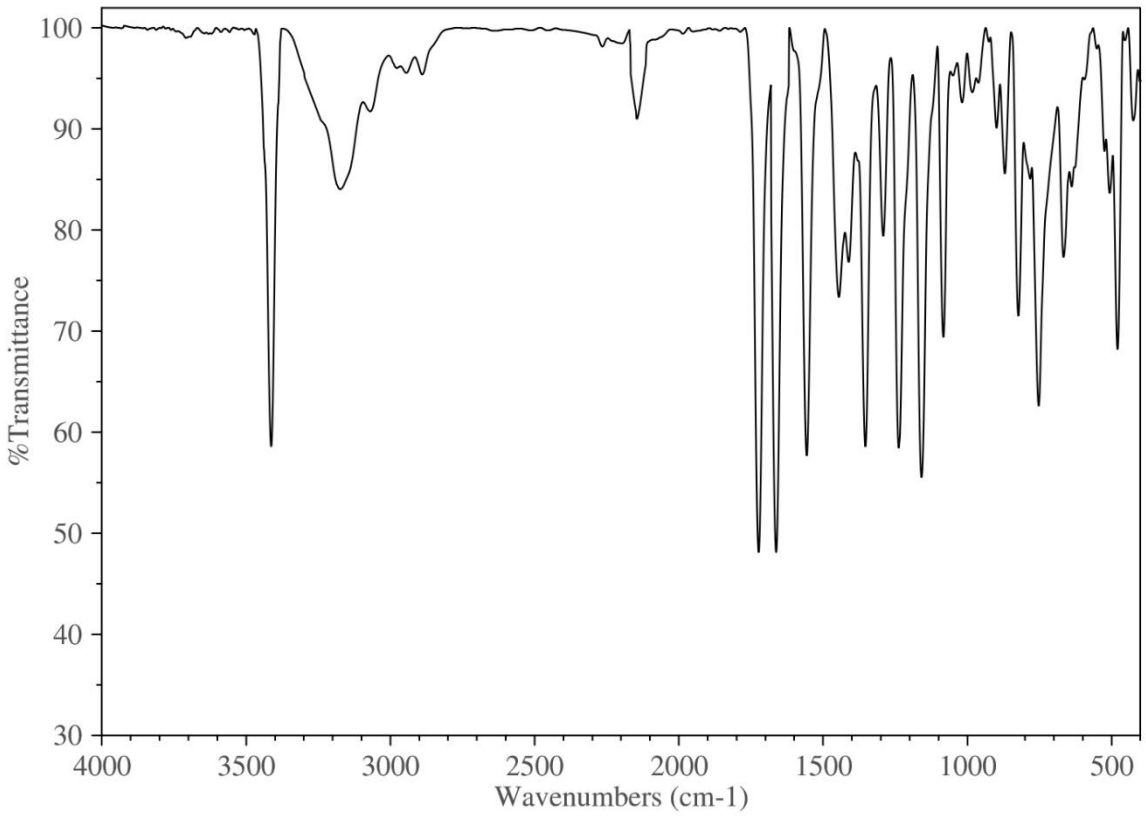

Figure S50. IR spectrum for compound **3e.**

```
Acq. Operator   : SYSTEM
Sample Operator : SYSTEM
Acq. Instrument : HPLC                              Location : Vial 25
Injection Date  : 6/1/2024 12:41:03 PM
                                                   Inj Volume : 5.000 µl
Acq. Method     : C:\CHEM32\1\METHODS\PURE.M
Last changed    : 6/1/2024 12:39:39 PM by SYSTEM
                  (modified after loading)
Analysis Method : C:\CHEM32\1\METHODS\DEF_LC.MCYANO COLUMN.M
Last changed    : 6/1/2024  1:30:41 PM by SYSTEM
                  (modified after loading)
Sample Info     : 50 ACN: 60 water, Flow 1.50 mL/min, 250 nm, 5 ul injection
```

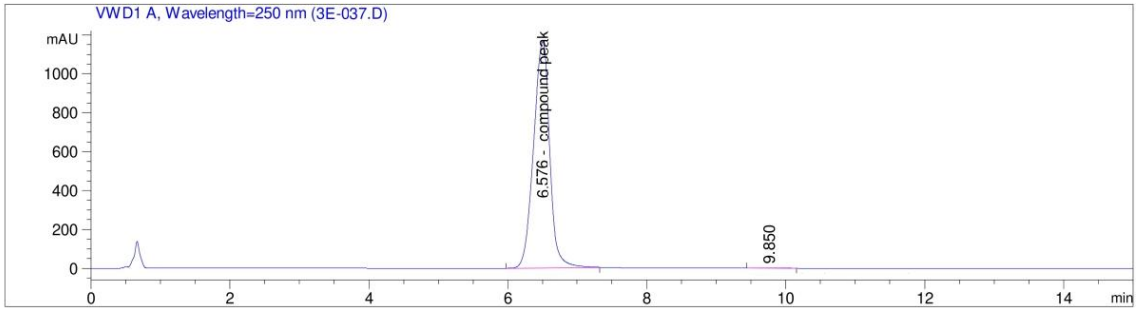


```
=====================================================================
                        Area Percent Report
=====================================================================

Sorted By             :      Signal
Calib. Data Modified  :      6/1/2024  1:30:41 PM
Multiplier            :      1.0000
Dilution              :      1.0000
Sample Amount:                :      1.00000  [ng/ul]   (not used in calc.)
Do not use Multiplier & Dilution Factor with ISTDs


Signal 1: VWD1 A, Wavelength=250 nm

Peak RetTime  Type   Width     Area      Area    Name
  #   [min]          [min]   [mAU*s]       %
----|-------|------|-------|----------|--------|---------------------
   1   6.576 BBA     0.2112 1.27192e4   97.5219 compound peak

Totals :                    1.27192e4   97.5219

                         *** End of Report ***
```

Figure 51. HPLC spectrum for compound **3e**.

Requester Data

Name:	**Haytham O. Tawfik**	Tel.	**01005356819**
Authority:	**Faculty of Pharmacy Tanta University**	Date	**13/07/2023**

Sample Data

Samples had been submitted for elemental analysis.

Analysis Report

No.	Code	C%	H%	N%	S%
1	**1**	65.89	3.95	10.98	12.55
2	**3a**	66.93	5.98	10.64	8.11
3	**3b**	69.04	4.75	10.39	8.02
4	**3c**	67.99	4.40	10.78	8.24
5	**3d**	60.84	3.51	9.16	7.05
6	**3e**	67.23	3.90	13.47	7.81
7	**3f**	66.89	4.48	9.83	7.42
8	**3g**	60.87	3.75	13.04	7.44
9	**3h**	65.91	4.58	9.99	7.71
10	**3i**	67.02	4.89	9.79	7.39
11	**3j**	56.89	3.90	11.94	13.82
12	**3k**	62.92	3.77	10.04	7.56
13	**3l**	56.42	3.43	8.96	6.84
14	**3m**	59.87	3.46	9.47	7.22
15	**3n**	58.09	3.29	9.18	7.02
16	**3o**	71.07	4.41	9.54	7.35
17	**3p**	62.34	3.63	12.69	14.44

Figure S52. Elemental analysis of intermediate **1** and targets **(3a-p)**.

Code	Found EI-MS (*m/z*)	Code	Found EI-MS (*m/z*) $[M]^+$
3a	393.04 $[M]^+$	**3i**	431.34 $[M]^+$
3b	401.03 $[M]^+$	**3j**	466.42 $[M]^+$
3c	387.41 $[M]^+$	**3k**	420.75 $[M]^+$ and 423.38 $[M+2]^+$
3d	455.27 $[M]^+$	**3l**	465.44 $[M]^+$ and 467.75 $[M+2]^+$
3e	412.12 $[M]^+$	**3m**	439.40 $[M]^+$ and 440.90 $[M+2]^+$
3f	429.35 $[M]^+$	**3n**	457.21 $[M]^+$ and 459.47 $[M+2]^+$
3g	432.04 $[M]^+$	**3o**	437.09 $[M]^+$
3h	417.35 $[M]^+$	**3p**	444.26 $[M]^+$

Figure S53. Mass results of targets **(3a-p)**.

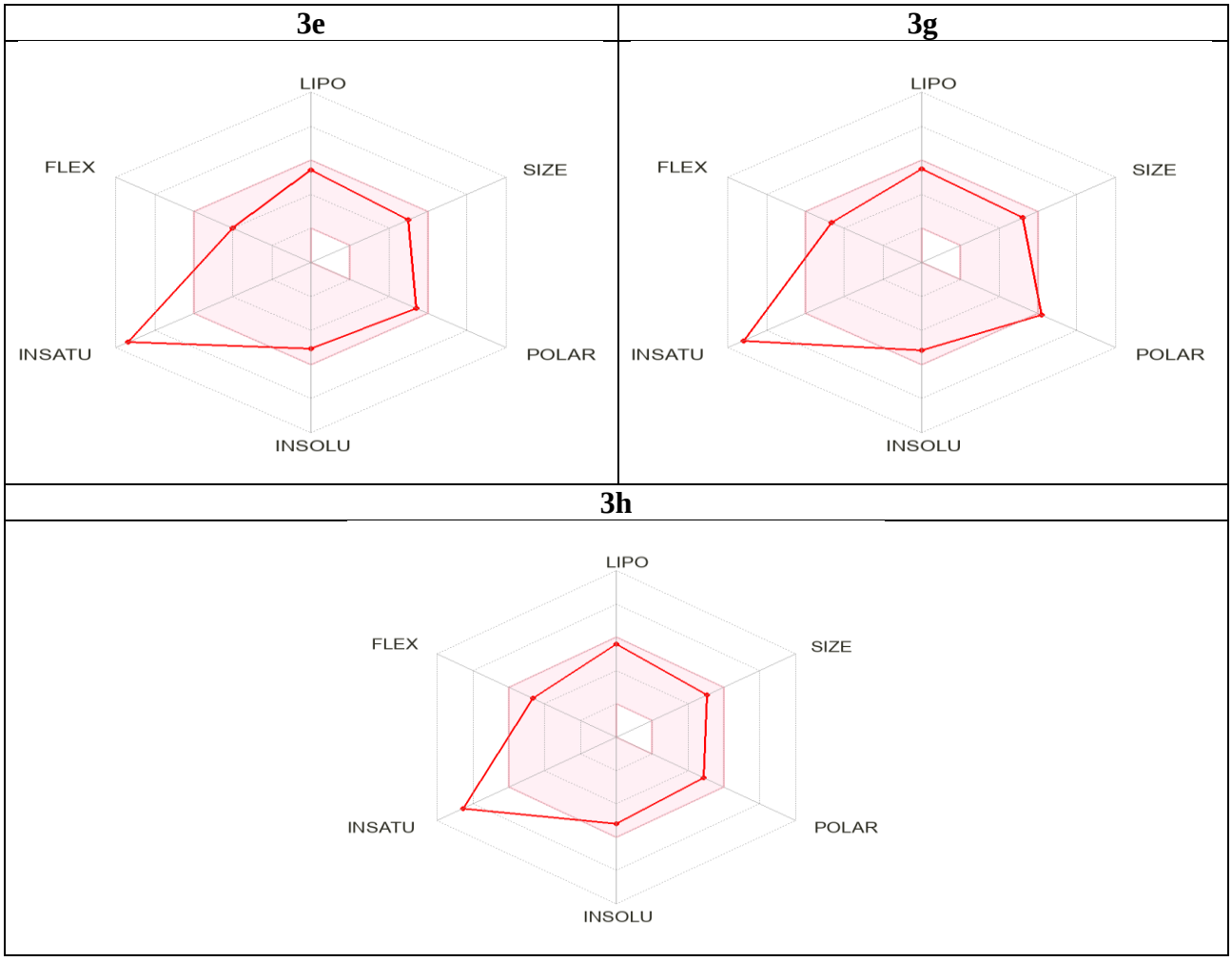

Figure S54. Radar bioavailability for studied compounds (**3e**, **3g**, and **3h**) in which the area in pink displays specific property optimal range. (LIPO = lipophilicity expressed as XLOGP3 (range from -0.7 to 5.0). SIZE= size expressed as molecular weight (range from 150 g/mol to 500 g/mol). POLAR = polarity expressed as TPSA (topological polar surface area) (range from 20 $Å^2$ to 130 $Å^2$). INSOLU = water insolubility by log S (ESOL) (range from -6 to 0). INSATU = insaturation expressed as for each carbons fraction in sp3 hybridization (range from 0.25 to 1). FLEX = flexibility, expressed as number of rotatable bonds (range from 0 to 9).

Materials and Methods

SI1. *In vitro* estimation of the inhibitory activity against acetylcholine esterase (AChE) and butyrylcholine esterase (BChE) enzymes

The assays were guided using a 96-well plate, as reported previously [1-4]. A microplate reader (Tecan, USA) and 96-well flat-bottom plates were used. Bovine serum albumin, enzymes (acetylcholinesterase (AChE) from electric eel (type VI-S lyophilized powder, EC 3.1.1.7) and horse butyrylcholinesterase (BChE) (EC 3.1.1.8)), substrates (acetylthiocholine, and butyrylthiocholine iodide) and indicator (Dithio-bis-(2-nitrobenzoic acid), DTNB)) were purchased from Sigma–Aldrich (St. Louis, MO, USA). Buffers and other chemicals were of extra pure analytical grade. In brief, 170 µL of Tris–HCl buffer (200 mM, pH 7.5), 20 µL at different concentrations of the tested compounds (125–1.953µg mL^{-1}), and 20 µL of the enzyme solution (0.1 U mL^{-1}) were subsequently added in the plates. After an incubation period of 10 min at 25 °C, 40 µL of indicator and 20 µL of the substrate (1.11 mM) were added. All samples were dissolved in DMSO. The intensity of the developed color was measured at 405 nm using a microplate reader (reading A) and control without the inhibitor was measured (reading B). Blank assays were performed by replacing the enzyme (20 µL) with buffer and their absorbances were recorded for correction of the spontaneous lysis of the indicator or inherent color of the inhibitor. All the reactions were performed in triplicate. Linear regression was performed for the calculation of the IC_{50} (50% inhibitory concentration). Microsoft Excel 2010 (Redmond, WA, USA) and GraphPad Instat 6.0 (Graphpad Software Inc., San Diego, CA) software were used for the data analysis where the % of inhibition was calculated according to the following equation.

$$.\%\ \text{Inhibition} = \left(1 - \frac{reading\ A}{reading\ B}\right) \times 100$$

SI2. Evaluation of antioxidant activity by DPPH radical scavenging method [5]

Free radical scavenging activity of the frontier target compounds (**3c**, **3e**, **3g**, and **3h**) was measured by 1, 1- diphenyl-2-picryl hydrazyl (DPPH). In brief, a 0.1 mM solution of DPPH in ethanol was prepared. This solution (1 mL) was added to 3 mL of different compounds in ethanol at different concentrations (3.9, 7.8, 15.62, 31.25, 62.5, 125, 250, 500, 1000 µg/mL). Here, only those compounds are used that are solubilized in ethanol and their various concentrations were prepared by dilution method. The mixture

was shaken vigorously and allowed to stand at room temperature for 30 min. Then, absorbance was measured at 517 nm by using a spectrophotometer (UV-VIS milton roy). The reference standard compound being used was ascorbic acid and the experiment was done in triplicate. The IC_{50} value of the sample, which is the concentration of sample required to inhibit 50% of the DPPH free radical, was calculated using the Log dose inhibition curve. The lower absorbance of the reaction mixture indicated higher free radical activity. The percent DPPH scavenging effect was calculated by using the following equation:

$$\text{DPPH scavenging effect (\%) or percent inhibition} = A_0 - A_1 / A_0 \times 100.$$

Where A_0 was the absorbance of the control reaction and A_1 was the absorbance in the presence of a test or standard sample.

SI3. Molecular dynamics simulations

The molecular dynamics simulations were carried out using the Desmond simulation package of Schrödinger LLC.[6-8] The NPγT ensemble with the temperature 300 K and a pressure of 1.01 bar was applied in all runs. The simulation length was 100 ns with a relaxation time of 1 ps. The OPLS4 force field parameters were used in all simulations.[9] The cutoff radius in Coulomb interactions was 9.0 Å. The orthorhombic periodic box boundaries were set 10 Å away from the protein atoms. The water molecules were explicitly described using the transferable intermolecular potential with the three points (TIP3P) model.[10] Salt concentration was set to 0.15 M NaCl and was built using the System Builder utility of Desmond. The Martyna−Tuckerman−Klein chain coupling scheme with a coupling constant of 2.0 ps was used for the pressure control and the Nosé−Hoover chain coupling scheme for the temperature control.[11, 12] Nonbonded forces were calculated using a RESPA integrator where the short-range forces were updated every step, and the long-range forces were updated every three steps. The trajectories were saved at 300 ps intervals for analysis. The behavior and interactions between the ligands and protein were analyzed using the Simulation Interaction Diagram tool implemented in the Desmond MD package. The stability of MD simulations was monitored by looking at the RMSD of the ligand and protein atom positions as a function of simulation time.

References

1. R. A. El-Shiekh, D. E. Ali, A. A. Mandour and M. R. Meselhy, *Industrial Crops and Products*, 2024, **221**, 119316.
2. A. F. Kassem, M. A. Omar, A. Temirak, R. A. El-Shiekh and A. M. Srour, *Future Medicinal Chemistry*, 2024, 1-17.
3. D. H. Dawood, A. M. Srour, M. A. Omar, T. A. Farghaly and R. A. El-Shiekh, *Archiv der Pharmazie*, 2024, **357**, 2300201.
4. M. A. Omar, R. A. El-Shiekh, D. H. Dawood, A. Temirak and A. M. Srour, *Future Medicinal Chemistry*, 2023, **15**, 2269-2287.
5. S. Kauthale, S. Tekale, M. Damale, J. Sangshetti and R. Pawar, *Bioorganic & Medicinal Chemistry Letters*, 2017, **27**, 3891-3896.
6. K. J. Bowers, D. E. Chow, H. Xu, R. O. Dror, M. P. Eastwood, B. A. Gregersen, J. L. Klepeis, I. Kolossvary, M. A. Moraes, F. D. Sacerdoti, J. K. Salmon, Y. Shan and D. E. Shaw, 2006.
7. M. H. El-Shershaby, A. Ghiaty, A. H. Bayoumi, A. A. Al-Karmalawy, E. M. Husseiny, M. S. El-Zoghbi and H. S. Abulkhair, *Bioorganic & Medicinal Chemistry*, 2021, **42**, 116266.
8. D. E. S. Research, *Journal*, 2021.
9. E. Harder, W. Damm, J. Maple, C. Wu, M. Reboul, J. Y. Xiang, L. Wang, D. Lupyan, M. K. Dahlgren, J. L. Knight, J. W. Kaus, D. S. Cerutti, G. Krilov, W. L. Jorgensen, R. Abel and R. A. Friesner, *Journal of Chemical Theory and Computation*, 2016, **12**, 281-296.
10. W. L. Jorgensen, J. Chandrasekhar, J. D. Madura, R. W. Impey and M. L. Klein, *Journal of Chemical Physics*, 1983, **79**, 926-935.
11. G. J. Martyna, M. L. Klein and M. Tuckerman, *Journal of Chemical Physics*, 1992, **97**, 2635-2643.
12. G. J. Martyna, D. J. Tobias and M. L. Klein, *Journal of Chemical Physics*, 1994, **101**, 4177-4189.